Chemical Engineering Science 66 (2011) 2177–2190

Contents lists available at ScienceDirect

Chemical Engineering Science

journal homepage: www.elsevier.com/locate/ces

# On diffusion, dispersion and reaction in porous media

F.J. Valdés-Parada *, C.G. Aguilar-Madera, J. Álvarez-Ramírez

*División de Ciencias Básicas e Ingeniería, Universidad Autónoma Metropolitana-Iztapalapa, Apartado Postal 55-534, 09340 México D.F., Mexico*

ARTICLE INFO

*Article history:*
Received 1 September 2010
Received in revised form
15 December 2010
Accepted 10 February 2011
Available online 25 February 2011

*Keywords:*
Effective diffusivity
Total dispersion tensor
Effective reaction rate coefficient
Upscaling
Volume averaging
Closure problem

ABSTRACT

The upscaling process of mass transport with chemical reaction in porous media is carried out using the method of volume averaging under diffusive and dispersive conditions. We study cases in which the (first-order) reaction takes place in the fluid that saturates the porous medium or when the reaction occurs at the solid–fluid interface. The upscaling process leads to average transport equations, which are expressed in terms of effective medium coefficients for (diffusive or dispersive) mass transport and reaction that are computed by solving the associated closure problems. Our analysis shows that these effective coefficients depend, in general, upon the nature and magnitude of the microscopic reaction rate as well as of the essential geometrical structure of the solid matrix and the flow rate. This study also shows that if the reaction rate at the microscale is arbitrarily large, the capabilities of the upscaled models are hindered, which is in agreement with the breakdown of the physical sense of the microscale formulation.



## 1. Introduction

Theoretical and experimental studies of effective transport properties under reactive and non-reactive conditions have taken great interest in the literature for, at least, the last 40 years. This is motivated by the broad range of scientific and engineering applications in which these processes take place. To quote some examples: chemical reaction engineering, groundwater hydrology, bacterial chemotaxis, and kinetics of crystallization process (cf. Levenspiel, 1999; Rushton, 2003; Valdés-Parada et al., 2009; Sperling, 2006). All these examples involve transport across several levels of scale, thus requiring a systematic flow of information from the smaller to the larger scales; this process is usually known as *upscaling* (Bear, 1972; Whitaker, 1999; Wood, 2009). Upscaled models involve the use of macroscopic equations containing effective transport parameters such as the effective diffusivity as well as the dispersion and reaction rate coefficients. It is clear that the success in representing transport phenomena in these hierarchical systems relies upon the accuracy to predict such effective parameters. In this respect, Lichtner and Kang (2007) recently solved reactive transport models at the pore scale using the Lattice–Boltzmann method and showed that pore-scale models can be used to determine the most appropriate form of the continuum formulation in addition to provide the values of the associated effective medium coefficients.

The effective diffusivity and the dispersion coefficient, decoupled from reactive conditions, have been obtained from well-established experimental and theoretical techniques. For example, the method of volume averaging (Whitaker, 1999) has been used to successfully predict the effective diffusivity (Ryan et al., 1980) and the dispersion coefficient (Eidsath et al., 1983) from spatially periodic non-consolidated porous media. Whereas Baiker et al. (1982) presented the effective diffusivities of catalyst pellets by using three different measuring techniques. Nevertheless, under reactive conditions there is still an open problem related to whether the effective parameters depend or not upon the reaction rate. This issue has been manifested through different experimental and theoretical methodologies in the literature. Experimentally, Park and Kim (1984) determined the effective diffusivity for active catalysts of NaY and LiY under reactive and non-reactive conditions. They reported that the diffusivities measured under reaction conditions were one order of magnitude smaller than those measured under non-reactive conditions. These discrepancies were attributed to the fact that geometric factors take major importance under reactive conditions. It should be stressed that their conclusions are restricted to values of the Thiele modulus around 2. Posteriorly, opposite conclusions were reported by Kolaczkowski and Ullah (1989) arguing that the effective diffusivity of a component is of the same order of magnitude regardless of the chemical reaction. However, these authors suggested that the diffusivity of the reactant may have been influenced by the reaction. García-Ochoa and Santos (1994) carried out experiments in silica alumina to determine the effective diffusivity and reported that, under reactive conditions, the tortuosity is greater than the non-reactive case but of similar

* Corresponding author.
*E-mail address:* iqfv@xanum.uam.mx (F.J. Valdés-Parada).

0009-2509/$ - see front matter © 2011 Elsevier Ltd. All rights reserved.
doi:10.1016/j.ces.2011.02.016

value. These differences were attributed to the role played by the microporosity. It is worth noting that differences found in reported experimental values may be attributed to the intrinsic differences of each experimental setup as well as the different mathematical models used by the above cited authors to interpret the results.

Along with the experimental evidence, some theoretical and numerical studies have been utilized to address the issue of dependence of the effective transport coefficients with the reaction rate. For instance, Wakao and Smith (1964) suggested that the effective diffusivity is certainly a function of the reaction rate. Their conclusions were derived through material balances in a simple model of a bidisperse porous medium. However, the same authors accept that such model contains some unrealistic simplifications, hence, their procedure should be carefully applied under certain conditions. In addition, a method based upon equivalent pore networks has been frequently used for describing the effect of the microstructure and reaction over the effective diffusivity (Sharratt and Mann, 1987; Sahimi, 1988; McGreavy et al., 1992; Dadvar and Sahimi, 2007). By using different variants in the methodology, all these works agree qualitatively that the effective diffusivity is modified by the chemical reaction and by parameters related with the pore structure as the pore size distribution and the network connectivity. However, an opposite conclusion was given by Zhang and Seaton (1994) who found that the effective diffusivity, when defined appropriately, does not depend on the reaction rate. It is added that this assumption is valid only in monodisperse structures and in microparticles within bidisperse catalysts.

The effect of a chemical reaction over effective properties in non-porous systems has also been noted. For a chemically active solute in unidirectional laminar flow channel, Balakotaiah and Chang (1995) used the center manifold theorem of the theory of dynamical systems to determine the dependence of the effective transport coefficients. It is demonstrated that slow bulk reactions do not affect dispersion but a correction to the apparent kinetics may arise due to nonlinear interaction among reaction, diffusion and convection. On fast surface reaction, the Taylor–Aris dispersion coefficient is reduced by a factor from 4 to 7.1 depending on the type of developed flow. Posteriorly, Balakotaiah and Dommeti (1999) once again used the center manifold theorem to derive upscaled models for packed-bed catalytic reactors. With a linear reaction taking place in the solid, not only the dispersion coefficient, but also the effective velocity and the effective reaction rate coefficients were found to be functions of the particle Damköhler number (the same conclusion was found by Edwards et al., 1993; Mauri, 1991). In addition, in the case where the reaction rate kinetics is nonlinear, the effective parameters depend also on the local concentration.

Allaire and Raphael (2007) utilized the method of homogenization to upscale a convection–diffusion model with reaction and thus obtain a homogenized model when both the Péclet and Damköhler numbers are much greater than one. They concluded that the homogenized longitudinal diffusion–dispersion coefficient is a decreasing function of the reaction rate. The same conclusion was elucidated recently by Allaire et al. (2010) using a novel methodology based on a two-scale expansion with drift approach to obtain the dispersion tensor and the upscaled model. Recently, Valdés-Parada and Alvarez-Ramirez (2010) studied the process of diffusion with homogeneous first-order reaction in porous media using the method of volume averaging. They showed that the effective diffusivity is, in general, a function of the reaction rate and reduces to the molecular diffusion coefficient for sufficiently large values of the Thiele modulus.

Summing up, the majority of the works mentioned above agree in that effective parameters are affected by the existence of a chemical reaction. However, because of the inherent complexity associated to the pore structure and the non-linearity related to the reactivity of the system, it is difficult to set general conclusions about the magnitudes of these effects. All these show that further detailed experimental studies and theoretical developments are required in order to better understand the process of mass transport and reaction in multiscale systems.

In this work we continue the recent work by Valdés-Parada and Alvarez-Ramirez (2010), which dealt with diffusion and homogeneous reaction in porous media. Particularly, we are interested in the study of a reactive porous system which involves bulk or surface first-order irreversible reaction occurring under diffusive and convective regimes. By using the method of volume averaging we are able to rigorously derive the form of the effective medium model and, most importantly, to define and predict the effective parameters (i.e., the effective diffusivity and total dispersion tensors and the effective reaction rate coefficient) appearing in the upscaled models. To this end, the analysis is divided into two parts: firstly, in Section 2 we extend the previous work by Ryan (1983) about diffusion and heterogeneous reaction in porous media to cases in which the Thiele modulus is not much less than one. In Section 3, we retake the work of Valdés-Parada and Alvarez-Ramirez (2010) and the derivations in Section 2, for mass transport and reaction driven by diffusion and convection. Finally, in Section 4 we present the corresponding discussion and concluding remarks.

## 2. Upscaling diffusion with heterogeneous reaction

Let us consider a rigid and homogeneous porous medium that is fully saturated with one phase (the $\gamma$-phase), such as the one sketched in Fig. 1. We are interested in studying the mass transport and reaction of a chemical species $A$ through the system. As mentioned above, the first case to be studied in this work corresponds to diffusion with heterogeneous first-order reaction. The governing equations at the pore-scale (i.e., the microscale) are

$$\frac{\partial c_{A\gamma}}{\partial t} = \nabla \cdot (\mathcal{D}_\gamma \nabla c_{A\gamma}) \quad \text{in the } \gamma\text{-phase} \tag{1a}$$

$$-\mathbf{n}_{\gamma\kappa} \cdot \mathcal{D}_\gamma \nabla c_{A\gamma} = k c_{A\gamma}, \quad \text{at the } \gamma-\kappa \text{ interface} \tag{1b}$$

where $\mathcal{D}_\gamma$ is the molecular diffusion coefficient and $k$ is the heterogeneous reaction rate coefficient. The microscale formulation is completed with the corresponding boundary conditions at the macroscale boundaries

$$c_{A\gamma} = \mathcal{F}(\mathbf{r},t) \quad \text{at } A_{\gamma e} \tag{2}$$

and with the initial condition,

$$c_{A\gamma} = \mathcal{G}(\mathbf{r}) \quad \text{when } t = 0 \tag{3}$$

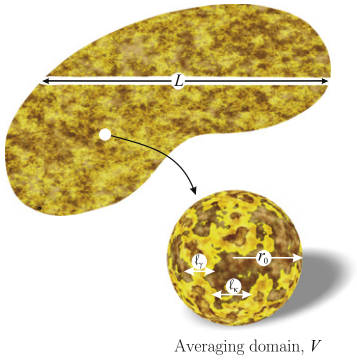


**Fig. 1.** Characteristic lengths of the system and sketch of the REV.

The upscaling process of this problem was first carried out by Ryan (1983) using the method of volume averaging (Whitaker, 1999). However, as mentioned above, his analysis was constrained to small values of the microscale Thiele modulus, which is defined by

$$\varphi_\mu = \sqrt{\frac{k\ell_\gamma}{\mathcal{D}_\gamma}} \tag{4}$$

here $\ell_\gamma$ is the characteristic length associated to the $\gamma$-phase (e.g., the pore diameter). In this section we revise this analysis without imposing such constraint. Since many of the steps of the upscaling process are available in the literature (see Whitaker, 1999, Chapter 1), we only present here those parts of the analysis where modifications are made. With this aim, let us introduce an averaging domain, $V$, or representative elementary volume (REV) (Bear, 1972) that contains portions of both phases as sketched in Fig. 1. The characteristic size of the REV, $r_0$, is usually constrained according to

$$\ell_\gamma \ll r_0 \ll L \tag{5}$$

with $L$ being the characteristic length associated to the macroscale. For a piecewise continuous function defined everywhere in the $\gamma$-phase, $\psi_\gamma$, let us introduce the *intrinsic averaging operator* as

$$\langle \psi_\gamma \rangle^\gamma = \frac{1}{\mathcal{V}} \int_{\mathbf{y}\in V_\gamma} \psi_\gamma \, dV(\mathbf{y}) \tag{6}$$

here $\mathcal{V}_\gamma$ is the domain occupied by the $\gamma$-phase in the REV. In this way, the volume fraction occupied by the fluid is defined as $\varepsilon_\gamma \equiv \mathcal{V}_\gamma/\mathcal{V}$.

Application of the intrinsic averaging operator to Eq. (1a), followed by proper exchange of differentiation and integration using the spatial averaging theorem (Howes and Whitaker, 1985), leads to

$$\frac{\partial \langle c_{A\gamma}\rangle^\gamma}{\partial t} = \nabla\cdot\left[\mathcal{D}_\gamma\left(\nabla\langle c_{A\gamma}\rangle^\gamma + \underbrace{\frac{1}{\mathcal{V}_\gamma}\int_{\mathbf{y}\in A_{\gamma\kappa}} \mathbf{n}_{\gamma\kappa}\tilde{c}_{A\gamma}\, dA(\mathbf{y})}_{\text{diffusion filter}}\right)\right] - \frac{a_v k}{\varepsilon_\gamma}\left(\langle c_{A\gamma}\rangle^\gamma + \underbrace{\frac{1}{\mathcal{A}_{\gamma\kappa}}\int_{\mathbf{y}\in A_{\gamma\kappa}} \tilde{c}_{A\gamma}\, dA(\mathbf{y})}_{\text{reaction filter}}\right) \tag{7}$$

where $a_v$ is the interfacial area per unit volume, i.e., $a_v = \mathcal{A}_{\gamma\kappa}/\mathcal{V}$ and $\tilde{c}_{A\gamma}$ represents the spatial deviations of the concentration with respect to the concentration intrinsic average (Gray, 1975),

$$\tilde{c}_{A\gamma} = c_{A\gamma} - \langle c_{A\gamma}\rangle^\gamma \tag{8}$$

It is worth stressing that the derivation of Eq. (7) involves neglecting the spatial variations of $\mathcal{D}_\gamma$ and $k$ within $V$. In addition, under the constraint in (5), it is reasonable to regard intrinsic averaged quantities as constants within the REV so that Eq. (7) is a *local* average equation. Furthermore, according to Quintard and Whitaker (1987) a porous medium is *homogeneous* with respect to a given REV when the effective transport coefficients are position-independent. This means that, under the assumption that the porous medium under consideration is homogeneous, it is justifiable to regard $\varepsilon_\gamma$ to be spatially stationary as done in Eq. (7).

Notice that two filters of information from the microscale have been identified in the above equation, i.e., one for diffusion and another for reaction; the latter is a consequence of not imposing that $\tilde{c}_{A\gamma} \ll \langle c_{A\gamma}\rangle^\gamma$ and this contrasts with the developments by Ryan (1983) where this assumption was made. In its current form, Eq. (7) is of little use since it is expressed in terms of the concentration deviations, which are unknown at this point. To overcome this issue, it is necessary to derive an expression for $\tilde{c}_{A\gamma}$ as a function of $\langle c_{A\gamma}\rangle^\gamma$ and its derivatives. This is usually known as the *closure process* (Whitaker, 1999) and it involves the following steps: (1) derive the governing equations and boundary conditions for the deviations fields, (2) impose a set of reasonable assumptions [or scaling laws in the sense of Wood (2009)] to simplify the problem and (3) derive the formal solution of the boundary-value problem. For brevity, the details related to the statement and solution of the closure problem are provided in Appendix A; here we only present its formal solution as

$$\tilde{c}_{A\gamma} = \mathbf{b}_\gamma\cdot\nabla\langle c_{A\gamma}\rangle^\gamma + s_\gamma\langle c_{A\gamma}\rangle^\gamma \tag{9}$$

with $\mathbf{b}_\gamma$ and $s_\gamma$ being the so-called *closure variables*, which are in turn integrals of Green's function associated to the boundary-value problem for the concentration deviations [see Eqs. (A.9)]. The closure variables solve the following boundary-value problems:

$$\nabla\cdot(\mathcal{D}_\gamma\nabla\mathbf{b}_\gamma) + \frac{k}{\mathcal{V}_\gamma}\int_{\mathbf{y}\in A_{\gamma\kappa}}\mathbf{b}_\gamma\, dA(\mathbf{y}) = \mathbf{0} \quad \text{in the } \gamma\text{-phase} \tag{10a}$$

$$-\mathbf{n}_{\gamma\kappa}\cdot\mathcal{D}_\gamma\nabla\mathbf{b}_\gamma = k\mathbf{b}_\gamma + \mathbf{n}_{\gamma\kappa}\mathcal{D}_\gamma \quad \text{at the } \gamma-\kappa \text{ interface} \tag{10b}$$

$$\mathbf{b}_\gamma(\mathbf{r}) = \mathbf{b}_\gamma(\mathbf{r}+\mathbf{l}_i), \quad i=1,2,3 \tag{10c}$$

$$\langle\mathbf{b}_\gamma\rangle^\gamma = \mathbf{0} \tag{10d}$$

$$\nabla\cdot(\mathcal{D}_\gamma\nabla s_\gamma) + \frac{k}{\mathcal{V}_\gamma}\int_{\mathbf{y}\in A_{\gamma\kappa}} s_\gamma\, dA(\mathbf{y}) = -\frac{a_v k}{\varepsilon_\gamma} \quad \text{in the } \gamma\text{-phase} \tag{11a}$$

$$-\mathbf{n}_{\gamma\kappa}\cdot\mathcal{D}_\gamma\nabla s_\gamma = k(s_\gamma+1) \quad \text{at the } \gamma-\kappa \text{ interface} \tag{11b}$$

$$s_\gamma(\mathbf{r}) = s_\gamma(\mathbf{r}+\mathbf{l}_i), \quad i=1,2,3 \tag{11c}$$

$$\langle s_\gamma\rangle^\gamma = 0 \tag{11d}$$

which result from substituting Eq. (9) into Eqs. (A.2), (A.3), (A.6) and (A.7). Notice that the fields of both closure variables depend upon the values of the reaction rate coefficient, $k$. To have a more clear idea of this functionality, we perform order of magnitude analyses to Eqs. (10b) and (11b), in order to obtain

$$\mathbf{b}_\gamma = \mathbf{O}\left(\frac{\ell_\gamma}{1+\varphi^2}\right), \quad s_\gamma = \mathbf{O}\left(\frac{\varphi^2}{1+\varphi^2}\right) \tag{12}$$

here $\varphi$ represents the cell Thiele modulus, defined as $\varphi = \sqrt{k\ell/\mathcal{D}_\gamma}$. Indeed, for values of $\varepsilon_\gamma$ that are close to 1, $\varphi = \mathbf{O}(\varphi_\mu)$. The closure problems were solved in a unit cell containing a square obstacle using the finite element solver Comsol Multiphysics 3.5a using adaptive mesh refinements to guarantee that the results are independent of the number of elements. It is stressed that periodic unit cell models are not necessarily constrained to the simple geometries here considered; in fact, models involving dead-end pores, as those analyzed by Lichtner and Kang (2007), may as well be used. From the estimates given in Eq. (12) and the results in Fig. 2 we notice that $\mathbf{b}_\gamma$ decreases rapidly with $\varphi$; in fact, it appears that $\varphi = 5$ is sufficient to reduce the fields of $\mathbf{b}_\gamma$ to practically zero. This can be explained from Eq. (10b), where we observe that for $\varphi \gg 1$, the problem becomes homogeneous and its solution is $\mathbf{b}_\gamma = \mathbf{0}$. These conditions correspond to cases such as separations involving homogeneous reversible reactions assumed at equilibrium as studied by Ochoa-Tapia et al. (1991). On the other hand, the $s_\gamma$-fields increase with the microscopic Thiele modulus as shown in Fig. 3. This increment is more plausible near the interfacial area as expected from Eq. (11b). In fact, from this expression, we observe that for $\varphi \gg 1$, $s_\gamma \to -1$ at $A_{\gamma\kappa}$, which is corroborated in Fig. 3(c).

Our next step in the analysis is to substitute Eq. (9) into Eq. (7) in order to obtain, after some algebraic rearrangements, the

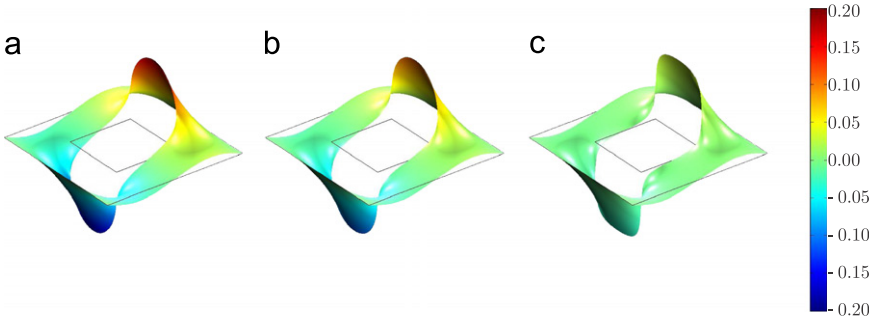


**Fig. 2.** Fields of the closure variable $(b_\gamma)_\kappa/\ell$ for $\varepsilon_\gamma = 0.8$ under different values of the Thiele modulus $\varphi$: (a) $\varphi = 1$, (b) $\varphi = 2$ and (c) $\varphi = 5$.

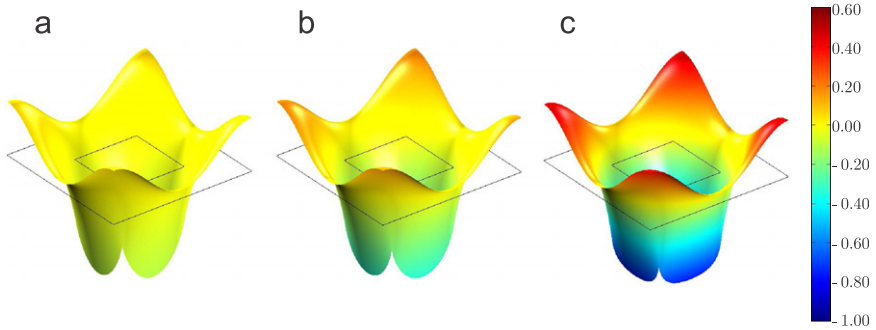


**Fig. 3.** Fields of the closure variable $s_\gamma$ for $\varepsilon_\gamma = 0.8$ under different values of the Thiele modulus $\varphi$: (a) $\varphi = 1$, (b) $\varphi = 2$ and (c) $\varphi = 5$.

following result:

$$\varepsilon_\gamma \frac{\partial \langle c_{A\gamma} \rangle^\gamma}{\partial t} = \nabla \cdot \left[ \varepsilon_\gamma \mathcal{D}_\gamma \left( \mathbf{I} + \frac{1}{\mathcal{V}_\gamma} \int_{\mathbf{y} \in A_{\gamma\kappa}} \mathbf{n}_{\gamma\kappa} \mathbf{b}_\gamma \, dA(\mathbf{y}) \right) \cdot \nabla \langle c_{A\gamma} \rangle^\gamma \right] - a_v k \left( 1 + \frac{1}{\mathcal{A}_{\gamma\kappa}} \int_{\mathbf{y} \in A_{\gamma\kappa}} s_\gamma \, dA(\mathbf{y}) \right) \langle c_{A\gamma} \rangle^\gamma - \left( \frac{k}{\mathcal{V}} \int_{\mathbf{y} \in A_{\gamma\kappa}} \mathbf{b}_\gamma \, dA(\mathbf{y}) - \frac{\mathcal{D}_\gamma}{\mathcal{V}} \int_{\mathbf{y} \in A_{\gamma\kappa}} \mathbf{n}_{\gamma\kappa} s_\gamma \, dA(\mathbf{y}) \right) \cdot \nabla \langle c_{A\gamma} \rangle^\gamma \tag{13}$$

However, on the basis of the estimates given in Eq. (12), we have that the order of magnitude of the last term in the above equation is

$$\left( \frac{k}{\mathcal{V}} \int_{\mathbf{y} \in A_{\gamma\kappa}} \mathbf{b}_\gamma \, dA(\mathbf{y}) - \frac{\mathcal{D}_\gamma}{\mathcal{V}} \int_{\mathbf{y} \in A_{\gamma\kappa}} \mathbf{n}_{\gamma\kappa} s_\gamma \, dA(\mathbf{y}) \right) \cdot \nabla \langle c_{A\gamma} \rangle^\gamma = \mathbf{O}\left( \frac{k \langle c_{A\gamma} \rangle^\gamma}{(1+\varphi^2)L} \right) \tag{14}$$

which turns out to be negligible with respect to

$$a_v k \langle c_{A\gamma} \rangle^\gamma = \mathbf{O}\left( \frac{k \langle c_{A\gamma} \rangle^\gamma}{\ell_\gamma} \right) \tag{15}$$

on the basis of the constraint $\ell_\gamma \ll (1+\varphi^2)L$. Notice that this constraint is easier to satisfy as $\varphi$ increases. In this way, it turns out that the diffusive filter only lets pass the closure variable $\mathbf{b}_\gamma$ while the reactive filter only allows the closure variable $s_\gamma$ to appear. Under these circumstances, Eq. (13) can be written as

$$\varepsilon_\gamma \frac{\partial \langle c_{A\gamma} \rangle^\gamma}{\partial t} = \nabla \cdot (\varepsilon_\gamma \mathbf{D}_{eff} \cdot \nabla \langle c_{A\gamma} \rangle^\gamma) - a_v k_{eff} \langle c_{A\gamma} \rangle^\gamma \tag{16}$$

where, we have introduced an effective diffusivity

$$\mathbf{D}_{eff} = \mathcal{D}_\gamma \left( \mathbf{I} + \frac{1}{\mathcal{V}_\gamma} \int_{\mathbf{y} \in A_{\gamma\kappa}} \mathbf{n}_{\gamma\kappa} \mathbf{b}_\gamma \, dA(\mathbf{y}) \right) \tag{17}$$

and an effective reaction rate coefficient

$$k_{eff} = k \left( 1 + \frac{1}{\mathcal{A}_{\gamma\kappa}} \int_{\mathbf{y} \in A_{\gamma\kappa}} s_\gamma \, dA(\mathbf{y}) \right) \tag{18}$$

This last equation contrasts with the work by Ryan (1983) (reproduced in Whitaker, 1999, Chapter 1), in which $k_{eff} = k$. As a matter of fact, the definition of $k_{eff}$ given in Eq. (18) is more general; certainly, for $\varphi \ll 1$, we have that $s_\gamma \to 0$ and thus $k_{eff} \to k$, which is consistent with the developments by Ryan. Despite the generality of Eq. (18), it is not convenient to use $k_{eff}$ for defining the macroscopic Thiele modulus ($\varphi_{Macro}$), since this is a dependent variable of $k$. Instead, one should follow Whitaker (1999) (see Eq. 1.4–33, p. 28) and define the macroscopic Thiele modulus as

$$\varphi_{Macro} = L \sqrt{a_v k / \mathcal{D}_\gamma} \tag{19}$$

In this way, combining Eqs. (19) and (4), we obtain

$$\varphi_{Macro} = L \sqrt{\frac{a_v}{\ell_\gamma}} \varphi_\mu \tag{20}$$

which clearly shows that the relation between the macroscopic and the microscopic Thiele moduli is similar to Eq. (5) in Kechagia et al. (2002). In fact, as explained by these authors, as $\varphi_\mu$ increases, it is more difficult to satisfy the assumption that upscaled variables change slowly at the microscale. Consequently, both microscale and macroscale model results in leading to non-local models.

Due to the dependence of the closure variables with $k$, it follows that both $\mathbf{D}_{eff}$ and $k_{eff}$ depend, in general, of the Thiele modulus as shown in Fig. 4 for two types of unit cells in 2D and 3D. It is interesting to notice that all the predictions for $k_{eff}/k$ seem to collapse in a single curve. This is due to the fact that the definition of this coefficient [see Eq. (18)] does not include $a_v$. In

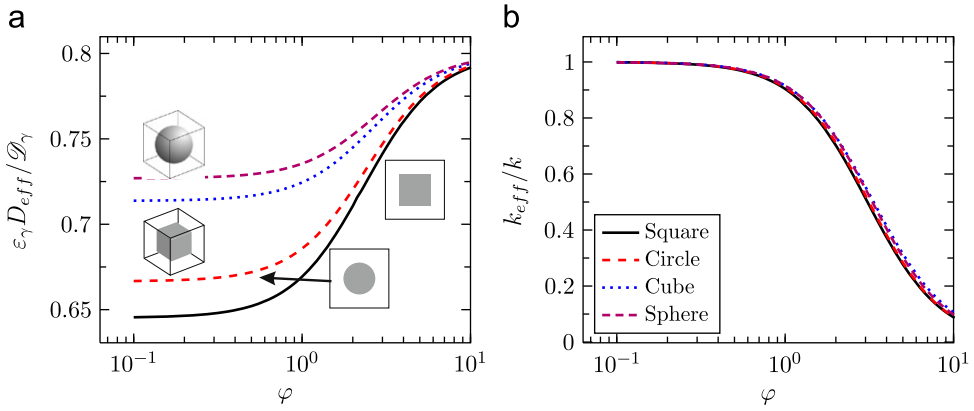


**Fig. 4.** (a) Effective diffusivity and (b) reaction rate coefficients as functions of the Thiele modulus $\varphi$ for $\varepsilon_\gamma = 0.8$ using 2D and 3D unit cells.

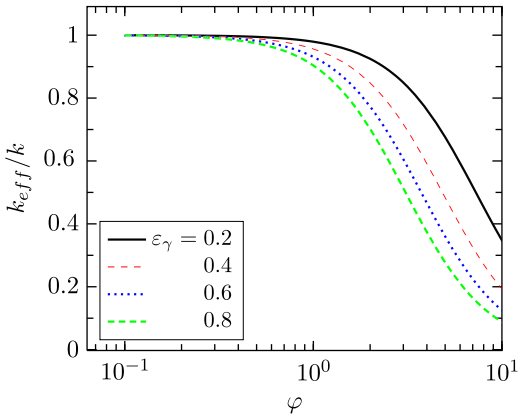


**Fig. 5.** Dependence of $k_{eff}/k$ with the porosity and $\varphi$ using 2D unit cells with a squared obstacle.

**Table 1**
Coefficients involved in Eq. (21).

| $\varepsilon_\gamma$ | 0.1 | 0.2 | 0.3 | 0.4 | 0.5 | 0.6 | 0.7 | 0.8 | 0.9 |
|---|---|---|---|---|---|---|---|---|---|
| $x_0$ | 10.6082 | 7.2580 | 5.7407 | 4.8247 | 4.1960 | 3.7312 | 3.3702 | 3.0833 | 2.8734 |
| $p$ | 1.9754 | 1.9611 | 1.9564 | 1.9582 | 1.9638 | 1.9710 | 1.9781 | 1.9846 | 1.9906 |

other words, the predictions of $k_{eff}/k$ are functions of the fluid volume fraction but not of the dimensionality of the unit cell whereas $a_v k_{eff}/k$ depends upon both $\varepsilon_\gamma$ and the unit cell geometry. In Fig. 5 we show the functionality of $k_{eff}/k$ with the porosity and the Thiele modulus using a 2D unit cell consisting of a centered square. Since the same sigmoidal shape is obtained in all cases, we fit the results from the numerical simulations to the following logistic-type equation:

$$\frac{k_{eff}}{k} = \frac{1}{1+(\varphi/x_0)^p} \tag{21}$$

The values of the coefficients $x_0$ and $p$ depend on the porosity and are available in Table 1. In all the fittings, the correlation coefficient was above 0.999. The relevance of the algebraic expression given in Eq. (21) should be evident, since it only requires knowing the porosity of the medium. Despite the fact that the results have been obtained in relatively simple unit cell models, it has been shown in the literature (cf. Whitaker, 1999) that the coefficients arising from this type of representations well-reproduce, in many cases, experimental data from more complicated geometries.

It is interesting to note that the shape of the profiles for $k_{eff}$ resembles the one shown in Fig. 14 of Wood et al. (2000) for the analysis of diffusion and heterogeneous reaction near the catalytic surface. In addition, the dependence with the porosity exhibited in Fig. 5 is in agreement with Fig. 6 of Valdés-Parada et al. (2006) for transport and reaction between a microporous medium and a homogeneous fluid.

For the effective diffusivity we observe that the results from 3D unit cells are larger than those from 2D domains. In addition, notice that the use of circular (spherical) representations of the solid phase leads to larger values than those corresponding to square (cubic) inclusions. We observe that the most evident differences in the results take place for $\varphi < 10$, when this is not the case, all results collapse in a single curve. This last is in concordance with our observations made in Figs. 2 and 3: when $\varphi$ is sufficiently large for $\mathbf{b}_\gamma \to \mathbf{0}$ and $s_\gamma \to -1$, we have from Eqs. (17) and (18), that $\mathbf{D}_{eff} \to \mathcal{D}_\gamma \mathbf{I}$ and $k_{eff}/k \to 0$, respectively.

To finalize this section, it is opportune to compare our results with those recently reported by Valdés-Parada and Alvarez-Ramirez (2010). These authors considered diffusion with homogeneous first-order reaction in a homogeneous porous medium arriving at the following upscaled model:

$$\varepsilon_\gamma \frac{\partial \langle c_{A\gamma} \rangle^\gamma}{\partial t} = \nabla \cdot (\varepsilon_\gamma \mathbf{D}^{rx}_{eff} \cdot \nabla \langle c_{A\gamma} \rangle^\gamma) - \varepsilon_\gamma k_h \langle c_{A\gamma} \rangle^\gamma \tag{22}$$

where $\mathbf{D}^{rx}_{eff}$ and $k_h$ are a reaction-dependent diffusivity tensor and the homogeneous reaction rate coefficient, respectively. In their work, Valdés-Parada and Alvarez–Ramirez studied the dependence of $\mathbf{D}^{rx}_{eff}$ with a Thiele modulus, $\phi = \sqrt{k_h \ell^2/\mathcal{D}_\gamma}$, noting a similar functionality as the one shown in Fig. 4 for $\mathbf{D}_{eff}$ with $\varphi$. It is interesting to notice that both $\mathbf{D}_{eff}$ and $\mathbf{D}^{rx}_{eff}$ are defined in the same way [see Eq. (17) in this work and Eq. (15) in Valdés-Parada and Alvarez-Ramirez (2010)]. However, the structure of the boundary-value problems that determine the fields of the closure variables is what ultimately makes the differences between the two effective coefficients.

To have a more quantitative perspective of the above, in Fig. 6 we compare the predictions of the $xx$-components of $\mathbf{D}_{eff}$ and $\mathbf{D}^{rx}_{eff}$ as functions of both $\varphi$ and $\phi$ for several porosity values using 2D and 3D unit cells. In Figs. 6(c) and (d), the percent of difference is defined as

$$\%\ \text{Difference} = \frac{|D_{eff} - D^{rx}_{eff}|}{D_{eff}} \times 100\% \tag{23}$$

As expected, for $\varphi, \phi \ll 1$, the reactive diffusivities reduce to the passive effective diffusivity derived by Ryan (1983). In the

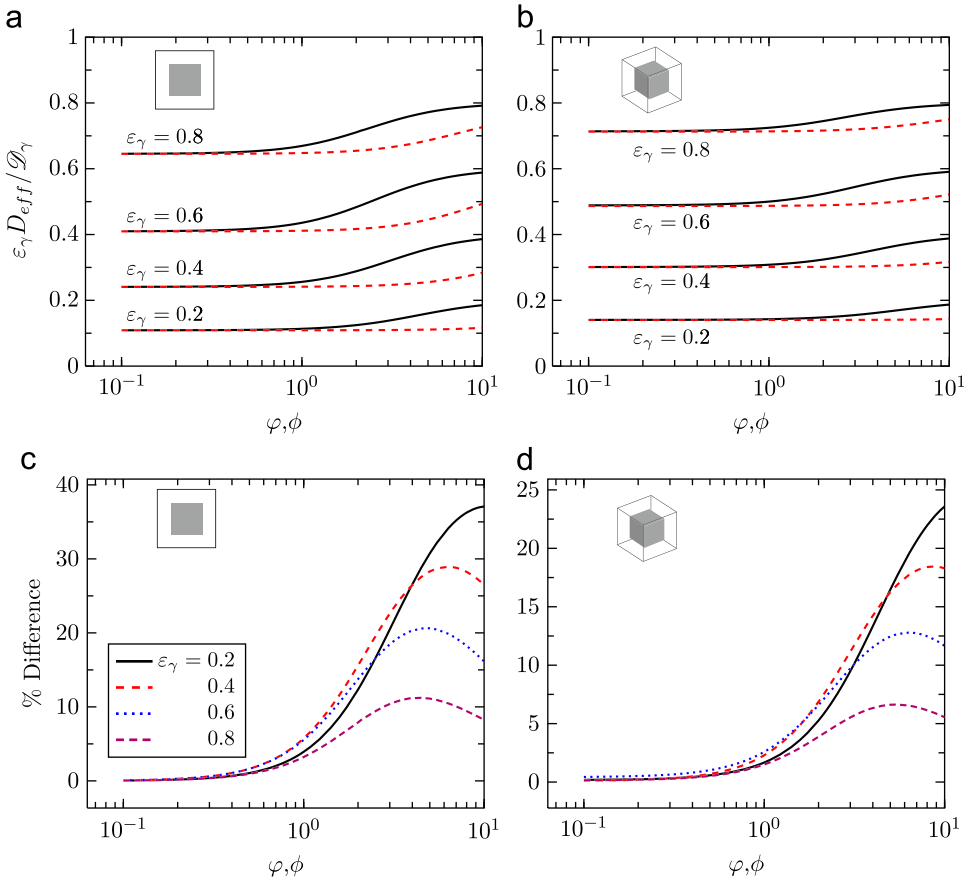


**Fig. 6.** Effective diffusivity and % differences between heterogeneous (—) and homogeneous (- - -) reaction models as functions of the Thiele moduli $\varphi$, $\phi$ using: 2D [(a) and (c)] and 3D [(b) and (d)] unit cells.

other extreme, when the Thiele moduli become considerably large (i.e., $\varphi,\phi \gg 1$), the values of both diffusivities tend to $\mathcal{D}_\gamma$. In this way, we find that, in general, the most important differences between the two models take place for values of the Thiele moduli around 10 [see Figs. 6(c) and (d)]. The magnitude of the maximum difference increases with the volume fraction of the solid phase reaching values as high as 40% for the case of 2D unit cell and $\varepsilon_\gamma = 0.2$.

The results from this section evidence that, regardless of the homogeneous or heterogeneous nature of the chemical reaction, the effective diffusivity is, in general, a function of the reaction rate. Moreover, the mathematical structure of the associated closure problems, as well as the geometry, is determinant in the particular type of dependence of the effective-medium coefficients. Certainly, this type of analysis should be extended to more complicated situations. For this reason, in the following section we study reactive dispersion in porous media involving homogeneous or heterogeneous reaction.

## 3. Dispersion and reaction

### 3.1. Homogeneous reaction

As an extension of our analysis of diffusive transport and reaction in porous media, we now study reactive dispersion. With this aim, let us first consider the process of diffusion and convection in a porous medium involving a homogeneous first-order chemical reaction taking place in the fluid phase. The governing differential equation at the microscale is in this case

$$\frac{\partial c_{A_\gamma}}{\partial t} + \nabla\cdot(\mathbf{v}_\gamma c_{A_\gamma}) = \nabla\cdot(\mathcal{D}_\gamma \nabla c_{A_\gamma}) - k_h c_{A_\gamma} \quad \text{in the } \gamma\text{-phase} \tag{24}$$

with $\mathbf{v}_\gamma$ being the fluid velocity, which is determined from the solution of the Navier–Stokes equations.

Assuming that the solid–fluid interface is impermeable to transport of species $A$, we have that

$$-\mathbf{n}_{\gamma\kappa}\cdot\mathcal{D}_\gamma\nabla c_{A_\gamma} = 0 \quad \text{at the } \gamma-\kappa \text{ interface} \tag{25}$$

In addition, the non-slip condition applies for the fluid velocity at $A_{\gamma\kappa}$. The details of the upscaling process for passive dispersion are available from Eidsath (1981). Since the extension to homogeneous reactive dispersion is straightforward, we only write here the unclosed equation that results from applying the spatial averaging operator together with the spatial averaging theorem and the corresponding spatial decompositions for the concentration and velocity; this is,

$$\varepsilon_\gamma \frac{\partial \langle c_{A_\gamma}\rangle^\gamma}{\partial t} + \nabla\cdot(\varepsilon_\gamma \langle \mathbf{v}_\gamma\rangle^\gamma \langle c_{A_\gamma}\rangle^\gamma) + \nabla\cdot\underbrace{\left(\varepsilon_\gamma \langle \tilde{\mathbf{v}}_\gamma \tilde{c}_{A_\gamma}\rangle^\gamma\right)}_{\text{dispersive filter}}$$
$$= \nabla\cdot\left[\varepsilon_\gamma \mathcal{D}_\gamma\left(\nabla\langle c_{A_\gamma}\rangle^\gamma + \underbrace{\frac{1}{\mathcal{V}_\gamma}\int_{\mathbf{y}\in A_{\gamma\kappa}} \mathbf{n}_{\gamma\kappa}\tilde{c}_{A_\gamma} dA(\mathbf{y})}_{\text{diffusive filter}}\right)\right]$$
$$-k_h\varepsilon_\gamma\langle c_{A_\gamma}\rangle^\gamma \tag{26}$$

where we have identified a diffusive and a dispersive filter, which will be responsible for capturing the essential information from the microscale. Following the tendency of the presentation in the

previous section, the derivation of the closure problem formal solution is provided in Appendix B. Here we summarize the result of this analysis into the following expression:

$$\tilde{c}_{A\gamma} = \mathbf{f}_{\gamma h} \cdot \nabla \langle c_{A\gamma} \rangle^{\gamma} \tag{27}$$

The closure variable, $\mathbf{f}_{\gamma h}$, solves the boundary-value problem

$$\tilde{\mathbf{v}}_{\gamma} + \mathbf{v}_{\gamma} \cdot \nabla \mathbf{f}_{\gamma h} = \nabla \cdot (\mathcal{D}_{\gamma} \nabla \mathbf{f}_{\gamma h}) - k_h \mathbf{f}_{\gamma h} \quad \text{in the } \gamma\text{-phase} \tag{28a}$$

$$-\mathbf{n}_{\gamma\kappa} \cdot (\mathcal{D}_{\gamma} \nabla \mathbf{f}_{\gamma h}) = \mathbf{n}_{\gamma\kappa} \mathcal{D}_{\gamma} \quad \text{at } A_{\gamma\kappa} \tag{28b}$$

$$\mathbf{f}_{\gamma h}(\mathbf{r}) = \mathbf{f}_{\gamma h}(\mathbf{r} + \mathbf{l}_i), \quad i = 1,2,3 \tag{28c}$$

$$\langle \mathbf{f}_{\gamma h} \rangle^{\gamma} = \mathbf{0} \tag{28d}$$

which results from substituting Eq. (27) into Eqs. (B.5). This problem was solved only for unit cells involving a square and a cubic obstacle, and similar results are obtained using the other geometrical configurations analyzed in the previous section. The simulations are presented for several values of the particle Péclet number, $Pe_p$, defined as

$$Pe_p = \frac{\| \langle \mathbf{v}_{\gamma} \rangle^{\gamma} \| d_p}{\mathcal{D}_{\gamma}} \left( \frac{\varepsilon_{\gamma}}{1 - \varepsilon_{\gamma}} \right) \tag{29}$$

here $d_p \equiv 6(\mathcal{V} - \mathcal{V}_{\gamma})/\mathcal{A}_{\gamma\kappa}$ is the equivalent particle diameter.

In Fig. 7 we show the sensitivity of the longitudinal (i.e., in the direction of the fluid flow) component of the vector $\mathbf{f}_{\gamma h}$ corresponding to changes in two orders of magnitude of the Thiele modulus, $\phi$, taking $Pe_p = 1$, 10 and 100, for a fixed volume fraction ($\varepsilon_{\gamma} = 0.8$). We observe that for $Pe_p = 1$ the results are driven by diffusion and reaction and they resemble those shown in Fig. 2. However, as the Péclet number is increased, convective transport competes with diffusion and chemical reaction. It is interesting to notice that for $\phi = 1$, 10, convection overcomes the other mechanisms if $Pe_p = 100$.

In order to close Eq. (26), we substitute Eq. (27) into the diffusive and dispersive filters to obtain

$$\varepsilon_{\gamma} \frac{\partial \langle c_{A\gamma} \rangle^{\gamma}}{\partial t} + \nabla \cdot (\varepsilon_{\gamma} \langle \mathbf{v}_{\gamma} \rangle^{\gamma} \langle c_{A\gamma} \rangle^{\gamma}) = \nabla \cdot (\varepsilon_{\gamma} \mathbf{D}_{\gamma}^{*,rx} \cdot \nabla \langle c_{A\gamma} \rangle^{\gamma}) - k_h \varepsilon_{\gamma} \langle c_{A\gamma} \rangle^{\gamma} \tag{30}$$

In this expression, the reaction term consists simply of the multiplication of $k_h$ with the porosity, which is consistent with the results by Valdés-Parada and Alvarez-Ramirez (2010) for diffusion with homogeneous reaction. In addition, we have introduced a total dispersion tensor that is dependent of the homogeneous reaction rate through the closure variable, $\mathbf{f}_{\gamma h}$, according to the following expression:

$$\mathbf{D}_{\gamma}^{*,rx} = \underbrace{\mathcal{D}_{\gamma} \left( \mathbf{I} + \frac{1}{\mathcal{V}_{\gamma}} \int_{\mathbf{y} \in A_{\gamma\kappa}} \mathbf{n}_{\gamma\kappa} \mathbf{f}_{\gamma h} \, dA(\mathbf{y}) \right)}_{\text{effective diffusion}} - \underbrace{\langle \tilde{\mathbf{v}}_{\gamma} \mathbf{f}_{\gamma h} \rangle^{\gamma}}_{\text{hydrodynamic dispersion}} \tag{31}$$

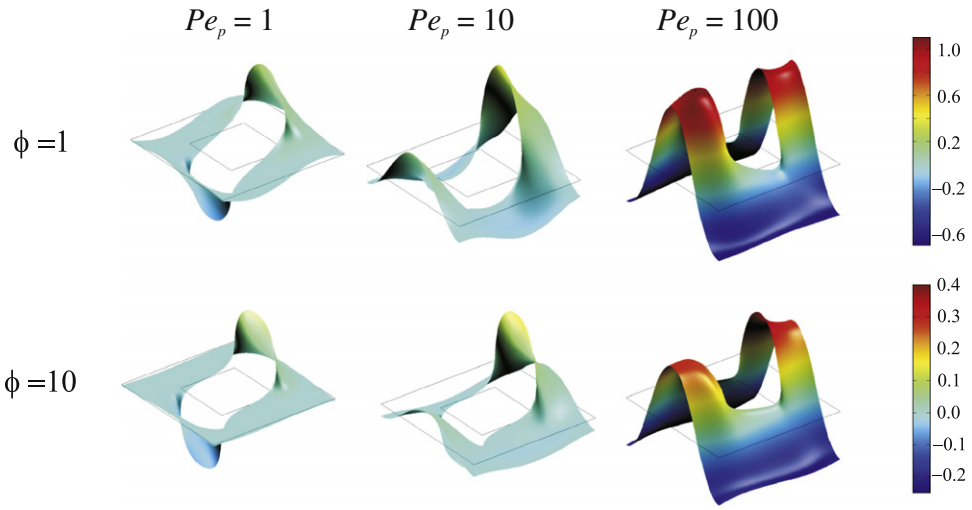


**Fig. 7.** Fields of the closure variable $(f_{\gamma h})_x/\ell$ for $\phi = 1$, 10 and $Pe_p = 1$, 10 and 100 for $\varepsilon_{\gamma} = 0.8$.

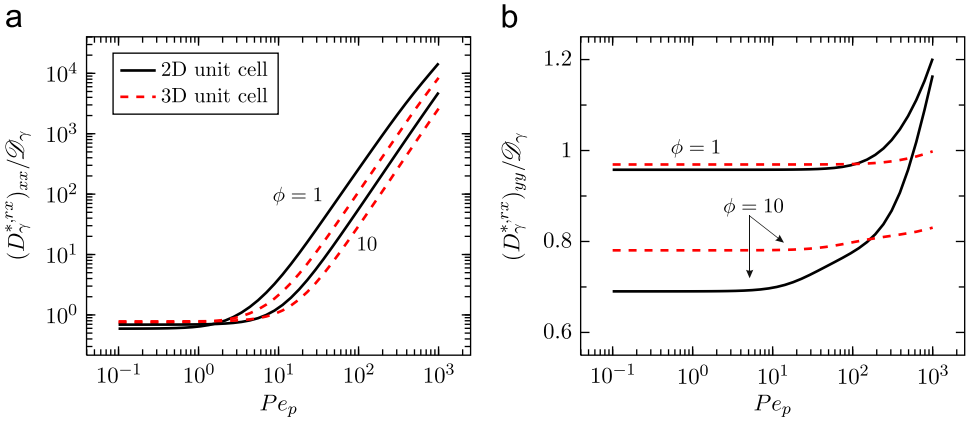


**Fig. 8.** (a) Longitudinal and (b) transverse components of the total dispersion tensor as a function of the Thiele modulus, $\phi$, and the particle Péclet number, $Pe_p$, for $\varepsilon_{\gamma} = 0.37$. The results were obtained using squared and cubic obstacles in the unit cells.

which encompasses the effects of diffusion and hydrodynamic dispersion. In Fig. 8 we plot the dependence of the longitudinal and transverse components of the total dispersion tensor for values of the Thiele modulus, $\phi$, ranging in two orders of magnitude. We observe that, contrary to the case of diffusion with (homogeneous and heterogeneous) reaction, an increment in the Thiele modulus leads to a decrement in the values of both components of the dispersion tensor. This is the consequence of the reactive term involved in the governing differential equation for the closure variable [i.e., Eq. (28a)], which competes with the convective transport contributions as explained above. According to our calculations, the results are insensitive to changes of the Thiele modulus whenever this parameter is smaller or equal to one. An interesting aspect of the predictions of the longitudinal and transverse dispersion coefficients is that for the first one, the results from 2D and 3D unit cells have the same trend for the range of $Pe_p$ values here considered. On the other hand, the profiles for the transverse dispersion differ more plausibly as $\phi$ is increased, especially for $Pe_p \gg 1$.

### 3.2. Heterogeneous reaction

The final case that we study corresponds to diffusion and convection in porous media involving a first-order chemical reaction at the solid–fluid interface. This process has been extensively studied in the literature using upscaling techniques such as extended Taylor dispersion theory (Edwards et al., 1993), homogenization (Mauri, 1991) and volume averaging (Wood et al., 2007). Our purpose here is to show the points in common between these approaches. The governing equations at the microscale are

$$\frac{\partial c_{A\gamma}}{\partial t}+\nabla\cdot(\mathbf{v}_\gamma c_{A\gamma})=\nabla\cdot(\mathcal{D}_\gamma\nabla c_{A\gamma}) \quad \text{in the } \gamma\text{-phase} \tag{32a}$$

$$-\mathbf{n}_{\gamma\kappa}\cdot\mathcal{D}_\gamma\nabla c_{A\gamma}=kc_{A\gamma} \quad \text{at the } \gamma-\kappa \text{ interface} \tag{32b}$$

Notice that the only difference between the above and Eqs. (1a)–(1b) is the inclusion of the convection transport term. For this reason, based on the derivations presented in Section 2, we can straightforwardly write the unclosed average model in the following form:

$$\begin{aligned}\varepsilon_\gamma\frac{\partial\langle c_{A\gamma}\rangle^\gamma}{\partial t}&+\nabla\cdot(\varepsilon_\gamma\langle c_{A\gamma}\rangle^\gamma\langle\mathbf{v}_\gamma\rangle^\gamma)\\&=\nabla\cdot\left[\varepsilon_\gamma\mathcal{D}_\gamma\left(\nabla\langle c_{A\gamma}\rangle^\gamma+\underbrace{\frac{1}{\mathcal{V}_\gamma}\int_{\mathbf{y}\in A_{\gamma\kappa}}\mathbf{n}_{\gamma\kappa}\tilde{c}_{A\gamma}dA(\mathbf{y})}_{\text{diffusive filter}}\right)-\underbrace{\varepsilon_\gamma\langle\tilde{c}_{A\gamma}\tilde{\mathbf{v}}_\gamma\rangle^\gamma}_{\text{dispersive filter}}\right]\\&\quad-ka_v\langle c_{A\gamma}\rangle^\gamma-\underbrace{\frac{k}{\mathcal{V}}\int_{\mathbf{y}\in A_{\gamma\kappa}}\tilde{c}_{A\gamma}\,dA(\mathbf{y})}_{\text{reactive filter}}\end{aligned} \tag{33}$$

Here we have identified three filters of the microscale information, namely the diffusive, dispersive and reactive filters. The developments in Appendix C show that the closure problem solution takes the following form:

$$\tilde{c}_{A\gamma}=\mathbf{f}_\gamma\cdot\nabla\langle c_{A\gamma}\rangle^\gamma+g_\gamma\langle c_{A\gamma}\rangle^\gamma \tag{34}$$

which is analogous to the one given in Eq. (9) for the case of diffusion with heterogeneous reaction. However, for the problem at hand, the closure variables $\mathbf{f}_\gamma$ and $g_\gamma$ also depend upon convection according to the following boundary-value problems:

$$\tilde{\mathbf{v}}_\gamma+\mathbf{v}_\gamma\cdot\nabla\mathbf{f}_\gamma=\nabla\cdot(\mathcal{D}_\gamma\nabla\mathbf{f}_\gamma)+\frac{k}{\mathcal{V}_\gamma}\int_{\mathbf{y}\in A_{\gamma\kappa}}\mathbf{f}_\gamma\,dA(\mathbf{y}) \tag{35a}$$

$$-\mathbf{n}_{\gamma\kappa}\cdot\mathcal{D}_\gamma\nabla\mathbf{f}_\gamma=k\mathbf{f}_\gamma+\mathbf{n}_{\gamma\kappa}\mathcal{D}_\gamma \quad \text{at the } \gamma-\kappa \text{ interface} \tag{35b}$$

$$\mathbf{f}_\gamma(\mathbf{r})=\mathbf{f}_\gamma(\mathbf{r}+\mathbf{l}_i),\quad i=1,2,3 \tag{35c}$$

$$\langle\mathbf{f}_\gamma\rangle^\gamma=\mathbf{0} \tag{35d}$$

$$\mathbf{v}_\gamma\cdot\nabla g_\gamma=\nabla\cdot(\mathcal{D}_\gamma\nabla g_\gamma)+\frac{ka_v}{\varepsilon_\gamma}+\frac{k}{\mathcal{V}_\gamma}\int_{\mathbf{y}\in A_{\gamma\kappa}}g_\gamma\,dA(\mathbf{y}) \tag{36a}$$

$$-\mathbf{n}_{\gamma\kappa}\cdot\mathcal{D}_\gamma\nabla g_\gamma=k(g_\gamma+1) \quad \text{at the } \gamma-\kappa \text{ interface} \tag{36b}$$

$$g_\gamma(\mathbf{r})=g_\gamma(\mathbf{r}+\mathbf{l}_i),\quad i=1,2,3 \tag{36c}$$

$$\langle g_\gamma\rangle^\gamma=0 \tag{36d}$$

which result from substituting Eq. (34) into Eqs. (C.3). The closed average model arises from substituting Eq. (34) into the filters present in Eq. (33); the resulting expression is

$$\begin{aligned}\varepsilon_\gamma\frac{\partial\langle c_{A\gamma}\rangle^\gamma}{\partial t}&+\nabla\cdot(\varepsilon_\gamma\langle c_{A\gamma}\rangle^\gamma\langle\mathbf{v}_\gamma\rangle^\gamma)\\&=\nabla\cdot\varepsilon_\gamma\left[\mathcal{D}_\gamma\left(\mathbf{I}+\frac{1}{\mathcal{V}_\gamma}\int_{\mathbf{y}\in A_{\gamma\kappa}}\mathbf{n}_{\gamma\kappa}\mathbf{f}_\gamma\,dA(\mathbf{y})\right)-\langle\mathbf{f}_\gamma\tilde{\mathbf{v}}_\gamma\rangle^\gamma\right]\cdot\nabla\langle c_{A\gamma}\rangle^\gamma\\&\quad-ka_v\langle c_{A\gamma}\rangle^\gamma\left[1+\frac{1}{\mathcal{A}_{\gamma\kappa}}\int_{\mathbf{y}\in A_{\gamma\kappa}}g_\gamma\,dA(\mathbf{y})\right]\\&\quad+\left[\frac{\mathcal{D}_\gamma}{\mathcal{V}}\int_{\mathbf{y}\in A_{\gamma\kappa}}\mathbf{n}_{\gamma\kappa}g_\gamma\,dA(\mathbf{y})-\frac{k}{\mathcal{V}}\int_{\mathbf{y}\in A_{\gamma\kappa}}\mathbf{f}_\gamma dA(\mathbf{y})-\varepsilon_\gamma\langle g_\gamma\tilde{\mathbf{v}}_\gamma\rangle^\gamma\right]\cdot\nabla\langle c_{A\gamma}\rangle^\gamma\end{aligned} \tag{37}$$

For brevity, in this part of the work, we do not present the fields of the closure variables since their dependence with $Pe_p$ and $\varphi$ can be inferred from the results in the previous examples. Moreover, as in the case of diffusion with heterogeneous reaction, order of magnitude analyses show that the last term of Eq. (37) plays a negligible role with respect to the others due to the length-scale constraint $\ell_\gamma \ll L$. Consequently, we may express the closed equation in the following more compact form:

$$\varepsilon_\gamma\frac{\partial\langle c_{A\gamma}\rangle^\gamma}{\partial t}+\nabla\cdot(\varepsilon_\gamma\langle c_{A\gamma}\rangle^\gamma\langle\mathbf{v}_\gamma\rangle^\gamma)=\nabla\cdot(\varepsilon_\gamma\mathbf{D}^*_\gamma\cdot\nabla\langle c_{A\gamma}\rangle^\gamma)-a_vk^*_{eff}\langle c_{A\gamma}\rangle^\gamma \tag{38}$$

which is the desired upscaled model, as it is expressed in terms of a total dispersion tensor, $\mathbf{D}^*_\gamma$, and an effective reaction rate coefficient, $k^*_{eff}$, which are defined as

$$\mathbf{D}^*_\gamma=\mathcal{D}_\gamma\left(\mathbf{I}+\frac{1}{\mathcal{V}_\gamma}\int_{\mathbf{y}\in A_{\gamma\kappa}}\mathbf{n}_{\gamma\kappa}\mathbf{f}_\gamma\,dA(\mathbf{y})\right)-\langle\mathbf{f}_\gamma\tilde{\mathbf{v}}_\gamma\rangle^\gamma \tag{39}$$

$$k^*_{eff}=k\left(1+\frac{1}{\mathcal{A}_{\gamma\kappa}}\int_{\mathbf{y}\in A_{\gamma\kappa}}g_\gamma\,dA(\mathbf{y})\right) \tag{40}$$

The above definitions have been previously reported by Wood et al. (2007) for the case in which a Michaelis–Menten kinetics can be approximated to a first-order expression (see Section 2.6 therein). Moreover, these authors proposed to interpret the ratio $k^*_{eff}/k$ as an effectiveness factor ($\eta$) and they analyzed the dependence of $\eta$ with the Damköhler number (i.e., $Da=\varphi^2$) for several Péclet number values (see Wood et al., 2007, Fig. 3). These authors noticed that $\eta$ is a decreasing function of $Da$ and this dependence was slightly altered by the Péclet number, especially for 3D unit cells. We verified these results, however for the sake of brevity we do not present them here since they are available elsewhere (i.e., Wood et al., 2007).

Furthermore, the derivations provided in this section are also in correspondence with those presented by Edwards et al. (1993) and Mauri (1991) using other upscaling techniques (i.e., generalized Taylor dispersion theory and homogenization, respectively).

The details of such correspondence are provided in Appendix D. Contrary to Wood et al. (2007), in the analysis of Edwards et al. (1993), the effective reaction rate is not regarded as an effectiveness factor; instead it is normalized in the form given in Eq. (D.10). In Fig. 9 we plot the normalized effective reaction rate coefficient with the Damköhler number taking Péclet number values ranging in four orders of magnitude. In addition, we have included the numerical results reported by Edwards et al. (1993) (see Table III therein); we observe, in general, good agreement between both approaches. The discrepancies are more plausible for $Da > 100$ and $Pe_p = 1$ for a square array of cylinders; this can be attributed to a number of sources such as the different definitions of the Péclet and Damköhler numbers, the different shapes of the obstacles involved in the unit cell, the number of mesh nodes in the numerical codes, among others. Despite these differences, it can be claimed that there is agreement from the results of both approaches. It is worth pointing out that the condition of fast kinetics in porous media involving mass transport driven by convection and diffusion was also studied by Kechagia et al. (2002) under a volume averaging framework. They found that if the reaction rate is fast, conventional volume averaging cannot be applied, except in the limit where the macroscale variables approach equilibrium. Under these conditions, the microscale and macroscale models are coupled through the associated closure problems needed to compute the effective medium coefficients. For situations far from equilibrium, nonlocal models are necessary.

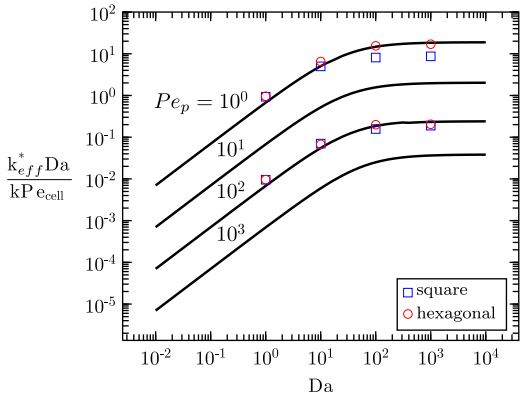


**Fig. 9.** Dependence of the effective reaction rate coefficient with *Da* for several particle Péclet number values using 2D unit cells with a squared obstacle taking $\varepsilon_\gamma = 0.37$ and comparison with the numerical results by Edwards et al. (1993) for square and hexagonal arrays of cylinders.

To finalize this section, in Fig. 10 we compare the predictions of the longitudinal component of the total dispersion tensor with those corresponding to the case involving homogeneous chemical reaction as functions of the particle Péclet number for Thiele moduli values changing in two orders of magnitude. Our results show that both dispersion coefficients are equally sensitive (qualitatively) to variations in the reaction rate. In addition, quantitative differences in the values of the dispersion coefficients can be appreciated for large values of the Thiele moduli, especially for 3D unit cells. Similar results are observed for the transverse component of the dispersion tensor and are not presented here for brevity.

## 4. Discussion and conclusions

In this work, we have carried out the upscaling of mass transport and (first-order) reaction processes, involving diffusion and convection, in porous media. Under a volume averaging framework, we have derived the corresponding effective medium equations in terms of average transport coefficients, which are, in turn, predicted by solving the associated closure problems in representative unit cells. Specifically, all models involved an effective (diffusive or dispersive) transport coefficient and an effective reaction rate coefficient. According to our simulations, the effective diffusion (or the total dispersion tensor in the case with convection) depends, in general, upon the reaction rate, independently of the (homogeneous or heterogeneous) nature of the reaction. Of course, the particular type of dependence is dictated by the type of reaction taking place as well as of the microstructure involved in the corresponding unit cell. Moreover, if the chemical reaction is homogeneous, the effective reaction rate coefficient is found to be simply the multiplication of $\varepsilon_\gamma k_h$, whereas if the reaction is heterogeneous, the fields of the effective reaction are determined from the solution of the associated closure problem.

An interesting feature of our analysis is that the effective diffusivity tends to the molecular diffusion for $\varphi \gg 1$; in addition, under the same circumstances, the cases involving heterogeneous reaction yield $k_{eff}/k \ll 1$. This means that the upscaled model seems to approach the governing equation for the fluid phase in the microscale (multiplied by the fluid volume fraction). However, it is actually very rare to find applications involving considerably large values of the microscopic (or even macroscopic) Thiele modulus. In fact, cases in which the transport terms are negligible with respect to the reaction rate term at the

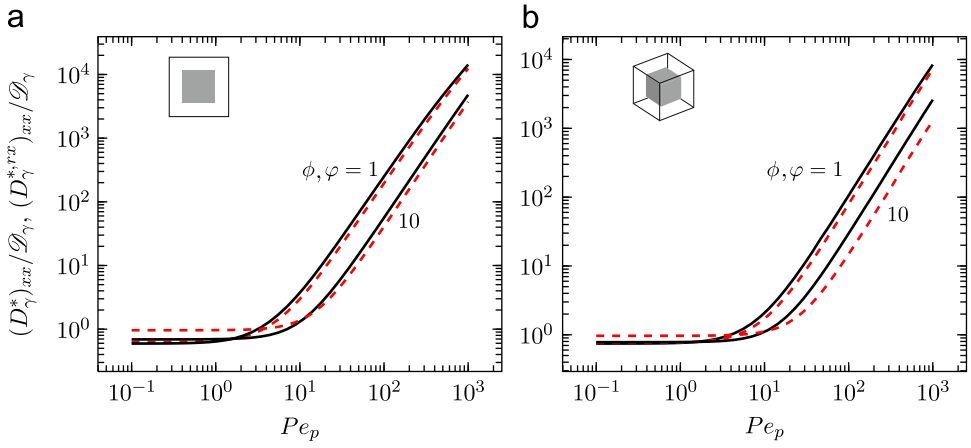


**Fig. 10.** Longitudinal dispersion coefficients involving heterogeneous (—) and homogeneous (- - -) reactions as functions of the particle Péclet number $Pe_p$ and the Thiele moduli, $\varphi$ and $\phi$ using (a) 2D and (b) 3D unit cells.

microscale may break the conservative nature of the mass balance formulation and hence the upscaling process. In other words, it does not make sense to upscale equations representing unphysical phenomena. This point of view is shared by Lichtner and Kang (2007), in their words. "It makes no sense at all to simply blindly average over a volume that contains large variations in concentration, for example, and thus by definition does not correspond to a REV".

It should be stressed that the results from this work are limited to first-order kinetics. This is a sensitive point since, for example if a zeroth-order reaction takes place in the fluid phase, no contribution from reaction arises in the closure problem. And thus, there is no reason for the effective transport coefficients to depend of the reaction rate in this case. Moreover, if the kinetics are non-linear, the solution of the closure problems becomes considerably more difficult and the structure of the upscaled model is not evident. Nevertheless, the derivations presented in this work, as well as the concordance with other upscaling techniques set the groundwork for future works dealing with reactive transport in porous media.

## Nomenclature

| | |
|---|---|
| $a_v$ | interfacial area per unit volume, $m^{-1}$ |
| $A_{\gamma e}$ | surface of entrances and exits |
| $A_{\gamma\kappa}$ | fluid–solid interface |
| $\mathcal{A}_{\gamma\kappa}$ | magnitude of the interfacial area within the averaging volume, $m^2$ |
| $\mathbf{b}_\gamma$ | closure variable associated with the macroscopic source $\boldsymbol{\nabla}\langle c_{A\gamma}\rangle^\gamma$ in the problem of diffusion with heterogeneous reaction, m |
| $c_{A\gamma}$ | concentration of chemical species $A$ in the fluid phase, $mol/m^3$ |
| $\langle c_{A\gamma}\rangle^\gamma$ | intrinsic average concentration of chemical species $A$, $mol/m^3$ |
| $\tilde{c}_{A\gamma}$ | spatial deviations of the concentration of chemical species $A$, $mol/m^3$ |
| $d_p$ | equivalent particle diameter, m |
| $\mathbf{D}_{eff}$ | effective diffusivity tensor under heterogeneous reaction, $m^2/s$ |
| $\mathbf{D}_{eff}^{rx}$ | effective diffusivity tensor under homogeneous reaction, $m^2/s$ |
| $\mathbf{D}_\gamma^*$ | total dispersion tensor under heterogeneous reaction, $m^2/s$ |
| $\mathbf{D}_\gamma^{*,rx}$ | total dispersion tensor under homogeneous reaction, $m^2/s$ |
| $\mathcal{D}_\gamma$ | molecular diffusion coefficient, $m^2/s$ |
| $\mathbf{f}_\gamma$ | closure variable associated with the macroscopic source $\boldsymbol{\nabla}\langle c_{A\gamma}\rangle^\gamma$ in the problem of dispersion with heterogeneous reaction, m |
| $\mathbf{f}_{\gamma h}$ | closure variable associated with the macroscopic source $\boldsymbol{\nabla}\langle c_{A\gamma}\rangle^\gamma$ in the problem of dispersion with homogeneous reaction, m |
| $G$ | Green's function associated to the closure problem solutions |
| $g_\gamma$ | closure variable associated with the macroscopic source $\langle c_{A\gamma}\rangle^\gamma$ in the problem of dispersion with heterogeneous reaction |
| $k$ | heterogeneous reaction rate coefficient, m/s |
| $k_h$ | homogeneous reaction rate coefficient, $s^{-1}$ |
| $k_{eff}$ | effective reaction rate coefficient under diffusive conditions, $s^{-1}$ |
| $k_{eff}^*$ | effective reaction rate coefficient under dispersive conditions, $s^{-1}$ |
| $L$ | characteristic length associated to the macroscale, m |
| $\mathbf{l}_i$ | lattice vector for periodic conditions, m |
| $\ell$ | length of the unit cell, m |
| $\ell_\gamma$ | characteristic length of the fluid phase, m |
| $\ell_\kappa$ | characteristic length of the solid phase, m |
| $\mathbf{n}_{\gamma\kappa}$ | unit normal vector pointing from the fluid to the solid phase |
| $p$ | fit parameter |
| $Pe_p$ | particle Péclet number |
| $\mathbf{r}$ | position vector, m |
| $r_0$ | characteristic size of the averaging volume, m |
| $s_\gamma$ | closure variable associated with the macroscopic source $\langle c_{A\gamma}\rangle^\gamma$ in the problem of diffusion with heterogeneous reaction |
| $t$ | time, s |
| $\mathbf{v}_\gamma$ | fluid velocity, m/s |
| $\langle\mathbf{v}_\gamma\rangle^\gamma$ | intrinsic average velocity of the fluid, m/s |
| $\tilde{\mathbf{v}}_\gamma$ | spatial deviations of the fluid velocity, m/s |
| $V$ | averaging domain or REV |
| $\mathcal{V}$ | magnitude of the averaging volume, $m^3$ |
| $V_\gamma$ | fluid portion within the averaging domain |
| $\mathcal{V}_\gamma$ | magnitude of the domain occupied by the fluid phase within the REV, $m^3$ |
| $\mathbf{y}$, $\mathbf{y}_0$ | position vectors, m |
| $x_0$ | fit parameter |

*Greek letters*

| | |
|---|---|
| $\varepsilon_\gamma$ | porosity |
| $\phi$ | microscale Thiele modulus with homogeneous reaction |
| $\varphi$ | microscale Thiele modulus with heterogeneous reaction |

## Acknowledgments

The authors want to express their gratitude to two anonymous reviewers, whose comments and suggestions helped improving the manuscript. F.J.V.P. thanks Prof. Brian Wood for his useful observations of our work.

## Appendix A. Closure problem for diffusion with heterogeneous reaction

In this section we state and formally solve the closure problem corresponding to diffusion with heterogeneous reaction. With this aim, let us commence by subtracting Eq. (7) to Eq. (1a), the resulting expression can be written as

$$\frac{\partial\tilde{c}_{A\gamma}}{\partial t}=\boldsymbol{\nabla}\cdot(\mathcal{D}_\gamma\boldsymbol{\nabla}\tilde{c}_{A\gamma})-\boldsymbol{\nabla}\cdot\left(\frac{\mathcal{D}_\gamma}{\mathcal{V}_\gamma}\int_{\mathbf{y}\in A_{\gamma\kappa}}\mathbf{n}_{\gamma\kappa}\tilde{c}_{A\gamma}\,dA(\mathbf{y})\right)+\underbrace{\frac{a_v k}{\varepsilon_\gamma}\langle c_{A\gamma}\rangle^\gamma}_{\text{volume reactive source}}+\frac{k}{\mathcal{V}_\gamma}\int_{\mathbf{y}\in A_{\gamma\kappa}}\tilde{c}_{A\gamma}\,dA(\mathbf{y})\quad\text{in the }\gamma\text{-phase}\tag{A.1}$$

In addition, the corresponding interfacial boundary condition arises from substituting the concentration spatial decomposition into Eq. (1b)

$$-\mathbf{n}_{\gamma\kappa}\cdot\mathcal{D}_\gamma\boldsymbol{\nabla}\tilde{c}_{A\gamma}=k\tilde{c}_{A\gamma}+\underbrace{k\langle c_{A\gamma}\rangle^\gamma}_{\text{surface reactive source}}+\underbrace{\mathbf{n}_{\gamma\kappa}\cdot\mathcal{D}_\gamma\boldsymbol{\nabla}\langle c_{A\gamma}\rangle^\gamma}_{\text{surface diffusive source}}\quad\text{at the }\gamma-\kappa\text{ interface}\tag{A.2}$$

At this point, it is opportune to point out that we have no intention on solving the closure problem in the entire macroscopic domain. If this were the case, the solution of the average model would actually be more complicated than solving the governing equations for $c_{A\gamma}$. According to Whitaker (1999), in portions of the porous medium that are not highly influenced by the transport processes taking place at the boundaries, it is reasonable to reduce the closure problem solution domain to a periodic representative zone of the microscale (i.e., a unit cell). In this way, one may adopt the following boundary condition at the entrances and exits:

$$\tilde{c}_{A\gamma}(\mathbf{r}) = \tilde{c}_{A\gamma}(\mathbf{r}+\mathbf{l}_i), \quad i=1,2,3 \tag{A.3}$$

The statement of the problem for $\tilde{c}_{A\gamma}$ is complete with the initial condition,

$$\tilde{c}_{A\gamma} = \tilde{\mathcal{G}}(\mathbf{r}), \quad \text{when } t=0 \tag{A.4}$$

which arises from substituting the concentration spatial decomposition into Eq. (3).

Before moving on, two simplifications are in order: (1) the closure problem can be treated as quasi-steady when $\partial\tilde{c}_{A\gamma}/\partial t \ll \nabla\cdot(\mathcal{D}_\gamma\nabla\tilde{c}_{A\gamma})$ and (2) the non-local diffusion term is usually negligible with respect to its local counterpart, i.e.,

$$\nabla\cdot\left(\frac{\mathcal{D}_\gamma}{\mathcal{V}_\gamma}\int_{\mathbf{y}\in A_{\gamma\kappa}}\mathbf{n}_{\gamma\kappa}\tilde{c}_{A\gamma}\,dA(\mathbf{y})\right) \ll \nabla\cdot(\mathcal{D}_\gamma\nabla\tilde{c}_{A\gamma}) \tag{A.5}$$

The time and length-scale constraints that support the above assumptions are $\ell_\gamma^2/\mathcal{D}_\gamma \ll t^*$ and $\ell_\gamma \ll L$, respectively. Under these circumstances, Eq. (A.1) reduces to

$$\nabla\cdot(\mathcal{D}_\gamma\nabla\tilde{c}_{A\gamma}) + \frac{k}{\mathcal{V}_\gamma}\int_{\mathbf{y}\in A_{\gamma\kappa}}\tilde{c}_{A\gamma}\,dA(\mathbf{y}) = \underbrace{-\frac{a_v k}{\varepsilon_\gamma}\langle c_{A\gamma}\rangle^\gamma}_{\text{volume reactive source}}$$

in the $\gamma$-phase (A.6)

Notice that in Eqs. (A.2) and (A.6) we have identified the volume and surface sources of deviations. In fact, these sources are responsible for making the $\tilde{c}_{A\gamma}$ fields to be different from the trivial solution. Comparing this formulation with the one originally presented by Ryan (1983), we observe that the only difference relies in the non-local reaction term in Eq. (A.6). Moreover, since we have disregarded the initial condition, it is necessary to impose the following integral constraint:

$$\langle\tilde{c}_{A\gamma}\rangle^\gamma = 0 \tag{A.7}$$

in order to set the levels of the concentration deviations.

Using standard Green's functions analysis and taking into account the time- and length-scale constraints already imposed, we find that the formal solution to this problem is given by

$$\begin{aligned}\tilde{c}_{A\gamma} = &\underbrace{\left(-\frac{a_v k}{\varepsilon_\gamma}\int_{\mathbf{y}_0\in V_\gamma} G(\mathbf{y},\mathbf{y}_0)dV(\mathbf{y}_0)\right)\langle c_{A\gamma}\rangle^\gamma}_{\text{influence of the volume reactive source}}\\ &\underbrace{-\left(\int_{\mathbf{y}_0\in A_{\gamma\kappa}} kG(\mathbf{y},\mathbf{y}_0)\,dA(\mathbf{y}_0)\right)\langle c_{A\gamma}\rangle^\gamma}_{\text{influence of the surface reactive source}}\\ &\underbrace{-\left(\int_{\mathbf{y}_0\in A_{\gamma\kappa}}\mathbf{n}_{\gamma\kappa}\mathcal{D}_\gamma G(\mathbf{y},\mathbf{y}_0)\,dA(\mathbf{y}_0)\right)\cdot\nabla\langle c_{A\gamma}\rangle^\gamma}_{\text{influence of the surface diffusive source}}\end{aligned} \tag{A.8}$$

where $G(\mathbf{y},\mathbf{y}_0)$ is the corresponding Green's function, which solves Eq. (A.6), with the right-hand side replaced by Dirac's delta function, subject to the homogeneous version of the boundary conditions for $\tilde{c}_{A\gamma}$. Notice that with this integral equation formulation, the role of each source is clearly identified in the solution. As a matter of convenience, let us introduce the following variables:

$$\mathbf{b}_\gamma(\mathbf{y}) = -\int_{\mathbf{y}_0\in A_{\gamma\kappa}}\mathbf{n}_{\gamma\kappa}\mathcal{D}_\gamma G(\mathbf{y},\mathbf{y}_0)\,dA(\mathbf{y}_0) \tag{A.9a}$$

$$s_\gamma(\mathbf{y}) = -\frac{a_v k}{\varepsilon_\gamma}\int_{\mathbf{y}_0\in V_\gamma} G(\mathbf{y},\mathbf{y}_0)\,dV(\mathbf{y}_0) - k\int_{\mathbf{y}_0\in A_{\gamma\kappa}} G(\mathbf{y},\mathbf{y}_0)\,dA(\mathbf{y}_0) \tag{A.9b}$$

so that Eq. (A.8) can be written in the form given by Eq. (9). Indeed, Green's functions can only be computed analytically for Chang's unit cell, as explained by Ochoa-Tapia et al. (1994). Furthermore, in this case, it is actually simpler to compute the fields of $\mathbf{b}_\gamma$ and $s_\gamma$ than those of $G(\mathbf{y},\mathbf{y}_0)$.

## Appendix B. Closure problem for dispersion with homogeneous reaction

In this section we derive and solve the closure problem associated to dispersion in porous media involving a homogeneous reaction. To this end, let us commence by rewriting Eq. (26) in the following form, on the basis of the homogeneity assumption of the porous medium,

$$\begin{aligned}&\frac{\partial\langle c_{A\gamma}\rangle^\gamma}{\partial t} + \nabla\cdot(\langle\mathbf{v}_\gamma\rangle^\gamma\langle c_{A\gamma}\rangle^\gamma) + \nabla\cdot\langle\tilde{\mathbf{v}}_\gamma\tilde{c}_{A\gamma}\rangle^\gamma\\ &\quad= \nabla\cdot\left[\mathcal{D}_\gamma\left(\nabla\langle c_{A\gamma}\rangle^\gamma + \frac{1}{\mathcal{V}_\gamma}\int_{\mathbf{y}\in A_{\gamma\kappa}}\mathbf{n}_{\gamma\kappa}\tilde{c}_{A\gamma}\,dA(\mathbf{y})\right)\right] - k_h\langle c_{A\gamma}\rangle^\gamma\end{aligned} \tag{B.1}$$

Recalling the definition of the concentration deviations, let us subtract the above equation to Eq. (24) in order to obtain

$$\begin{aligned}&\frac{\partial\tilde{c}_{A\gamma}}{\partial t} + \nabla\cdot(\tilde{\mathbf{v}}_\gamma\langle c_{A\gamma}\rangle^\gamma) + \nabla\cdot(\mathbf{v}_\gamma\tilde{c}_{A\gamma}) = \nabla\cdot(\mathcal{D}_\gamma\nabla\tilde{c}_{A\gamma}) - k_h\tilde{c}_{A\gamma}\\ &\quad-\nabla\cdot\left[\frac{\mathcal{D}_\gamma}{\mathcal{V}_\gamma}\int_{\mathbf{y}\in A_{\gamma\kappa}}\mathbf{n}_{\gamma\kappa}\tilde{c}_{A\gamma}\,dA(\mathbf{y}) - \langle\tilde{\mathbf{v}}_\gamma\tilde{c}_{A\gamma}\rangle^\gamma\right] \quad \text{in the } \gamma\text{-phase}\end{aligned} \tag{B.2}$$

The last two terms in the above equation represent non-local diffusion and convection and their orders of magnitude estimates are given by

$$\nabla\cdot\left[\frac{\mathcal{D}_\gamma}{\mathcal{V}_\gamma}\int_{\mathbf{y}\in A_{\gamma\kappa}}\mathbf{n}_{\gamma\kappa}\tilde{c}_{A\gamma}\,dA(\mathbf{y})\right] = \mathbf{O}\left(\frac{\mathcal{D}_\gamma\tilde{c}_{A\gamma}}{\ell_\gamma L}\right) \tag{B.3a}$$

$$\nabla\cdot\langle\tilde{\mathbf{v}}_\gamma\tilde{c}_{A\gamma}\rangle^\gamma = \mathbf{O}\left(\frac{\langle\mathbf{v}_\gamma\rangle^\gamma\tilde{c}_{A\gamma}}{L}\right) \tag{B.3b}$$

whereas the order of magnitude estimates of their local counterparts are

$$\nabla\cdot(\mathcal{D}_\gamma\nabla\tilde{c}_{A\gamma}) = \mathbf{O}\left(\frac{\mathcal{D}_\gamma\tilde{c}_{A\gamma}}{\ell_\gamma^2}\right) \tag{B.4a}$$

$$\nabla\cdot(\mathbf{v}_\gamma\tilde{c}_{A\gamma}) = \mathbf{O}\left(\frac{\langle\mathbf{v}_\gamma\rangle^\gamma\tilde{c}_{A\gamma}}{\ell_\gamma}\right) \tag{B.4b}$$

Therefore, due to the disparity between the characteristic lengths associated to the microscale and the macroscale (i.e., $\ell_\gamma \ll L$), we may simplify Eq. (B.2) to

$$\underbrace{\tilde{\mathbf{v}}_\gamma\cdot\nabla\langle c_{A\gamma}\rangle^\gamma}_{\text{convective source}} + \mathbf{v}_\gamma\cdot\nabla\tilde{c}_{A\gamma} = \nabla\cdot(\mathcal{D}_\gamma\nabla\tilde{c}_{A\gamma}) - k_h\tilde{c}_{A\gamma} \quad \text{in the } \gamma\text{-phase} \tag{B.5a}$$

here we have restrained the analysis to quasi-steady conditions and taken into account the fact that the fluid velocity and its deviations are solenoidal. Moreover, the interfacial boundary condition for $\tilde{c}_{A\gamma}$ arises from spatially decomposing the

concentration fields in Eq. (25) and can be written as

$$-\mathbf{n}_{\gamma\kappa}\cdot(\mathcal{D}_\gamma\nabla\tilde{c}_{A\gamma})=\underbrace{\mathbf{n}_{\gamma\kappa}\cdot(\mathcal{D}_\gamma\nabla\langle c_{A\gamma}\rangle^\gamma)}_{\text{diffusive source}}\quad\text{at } A_{\gamma\kappa} \tag{B.5b}$$

The closure problem is completed with the periodicity condition

$$\tilde{c}_{A\gamma}(\mathbf{r})=\tilde{c}_{A\gamma}(\mathbf{r}+\mathbf{l}_i),\quad i=1,2,3 \tag{B.5c}$$

and the average constraint for the deviation fields

$$\langle\tilde{c}_{A\gamma}\rangle^\gamma=0 \tag{B.5d}$$

In this case there are only diffusive and convective sources, however the reaction is intrinsically involved in the concentration deviation fields because of the last term on the right-hand side of Eq. (B.5a). In this way, the formal solution of the closure problem is

$$\begin{aligned}\tilde{c}_{A\gamma}=&\underbrace{\left(\int_{\mathbf{y}_0\in V_\gamma}G(\mathbf{y},\mathbf{y}_0)\tilde{\mathbf{v}}_\gamma\,dV(\mathbf{y}_0)\right)\cdot\nabla\langle c_{A\gamma}\rangle^\gamma}_{\text{influence of the convective source}}\\&\underbrace{-\left(\int_{\mathbf{y}_0\in A_{\gamma\kappa}}\mathbf{n}_{\gamma\kappa}\mathcal{D}_\gamma G(\mathbf{y},\mathbf{y}_0)\,dA(\mathbf{y}_0)\right)\cdot\nabla\langle c_{A\gamma}\rangle^\gamma}_{\text{influence of the surface diffusive source}}\end{aligned} \tag{B.6}$$

To simplify this result, let us introduce the following closure variable:

$$\mathbf{f}_{\gamma h}(\mathbf{y})=\int_{\mathbf{y}_0\in V_\gamma}G(\mathbf{y},\mathbf{y}_0)\tilde{\mathbf{v}}_\gamma\,dV(\mathbf{y}_0)-\int_{\mathbf{y}_0\in A_{\gamma\kappa}}\mathbf{n}_{\gamma\kappa}\mathcal{D}_\gamma G(\mathbf{y},\mathbf{y}_0)\,dA(\mathbf{y}_0) \tag{B.7}$$

which allows expressing Eq. (B.6) in the form given by Eq. (27) and this concludes the analysis.

## Appendix C. Closure problem for dispersion with heterogeneous reaction

In this case, the unclosed equation takes the following form:

$$\begin{aligned}&\frac{\partial\langle c_{A\gamma}\rangle^\gamma}{\partial t}+\nabla\cdot(\langle c_{A\gamma}\rangle^\gamma\langle\mathbf{v}_\gamma\rangle^\gamma)\\&\quad=\nabla\cdot\left[\mathcal{D}_\gamma\left(\nabla\langle c_{A\gamma}\rangle^\gamma+\frac{1}{\mathcal{V}_\gamma}\int_{\mathbf{y}\in A_{\gamma\kappa}}\mathbf{n}_{\gamma\kappa}\tilde{c}_{A\gamma}\,dA(\mathbf{y})\right)-\langle\tilde{c}_{A\gamma}\tilde{\mathbf{v}}_\gamma\rangle^\gamma\right]\\&\qquad-\frac{ka_v\langle c_{A\gamma}\rangle^\gamma}{\varepsilon_\gamma}-\frac{k}{\mathcal{V}_\gamma}\int_{\mathbf{y}\in A_{\gamma\kappa}}\tilde{c}_{A\gamma}\,dA(\mathbf{y})\end{aligned} \tag{C.1}$$

which results from dividing Eq. (37) by $\varepsilon_\gamma$ and assuming that the porous medium can be treated as homogeneous. Subtracting the above equation to Eq. (32a) leads to the following expression for the concentration deviations:

$$\begin{aligned}&\frac{\partial\tilde{c}_{A\gamma}}{\partial t}+\nabla\cdot(\tilde{\mathbf{v}}_\gamma\langle c_{A\gamma}\rangle^\gamma)+\nabla\cdot(\mathbf{v}_\gamma\tilde{c}_{A\gamma})\\&\quad=\mathcal{D}_\gamma\nabla^2\tilde{c}_{A\gamma}-\nabla\cdot\left[\frac{\mathcal{D}_\gamma}{\mathcal{V}_\gamma}\int_{\mathbf{y}\in A_{\gamma\kappa}}\mathbf{n}_{\gamma\kappa}\tilde{c}_{A\gamma}\,dA(\mathbf{y})-\langle\tilde{c}_{A\gamma}\tilde{\mathbf{v}}_\gamma\rangle^\gamma\right]\\&\qquad+\frac{ka_v\langle c_{A\gamma}\rangle^\gamma}{\varepsilon_\gamma}+\frac{k}{\mathcal{V}_\gamma}\int_{\mathbf{y}\in A_{\gamma\kappa}}\tilde{c}_{A\gamma}\,dA(\mathbf{y})\end{aligned} \tag{C.2}$$

Following the analysis in Appendix B, we have that, on the basis of the length-scale constraint $\ell_\gamma\ll L$, the non-local diffusion and convection terms can be assumed negligible with respect to their local counterparts. Therefore, restraining the analysis to quasi-steady conditions, we have that the concentration deviations solve the differential equation

$$\begin{aligned}&\underbrace{\tilde{\mathbf{v}}_\gamma\cdot\nabla\langle c_{A\gamma}\rangle^\gamma}_{\text{convective source}}+\mathbf{v}_\gamma\cdot\nabla\tilde{c}_{A\gamma}=\nabla\cdot(\mathcal{D}_\gamma\nabla\tilde{c}_{A\gamma})+\underbrace{\frac{ka_v\langle c_{A\gamma}\rangle^\gamma}{\varepsilon_\gamma}}_{\text{volume reactive source}}\\&\quad+\frac{k}{\mathcal{V}_\gamma}\int_{\mathbf{y}\in A_{\gamma\kappa}}\tilde{c}_{A\gamma}\,dA(\mathbf{y})\end{aligned} \tag{C.3a}$$

where the solenoidal properties of the velocity and its deviations have been taken into account. The interfacial boundary condition arises from the substitution of the concentration deviations into Eq. (32b), the result can be written as follows:

$$\begin{aligned}&-\mathbf{n}_{\gamma\kappa}\cdot\mathcal{D}_\gamma\nabla\tilde{c}_{A\gamma}=k\tilde{c}_{A\gamma}+\underbrace{k\langle c_{A\gamma}\rangle^\gamma}_{\text{surface reactive source}}+\underbrace{\mathbf{n}_{\gamma\kappa}\cdot\mathcal{D}_\gamma\nabla\langle c_{A\gamma}\rangle^\gamma}_{\text{diffusive source}},\\&\text{at the }\gamma-\kappa\text{ interface}\end{aligned} \tag{C.3b}$$

To complete the closure problem statement, we impose the periodicity condition at the entrances and exits of the unit cell

$$\tilde{c}_{A\gamma}(\mathbf{r})=\tilde{c}_{A\gamma}(\mathbf{r}+\mathbf{l}_i),\quad i=1,2,3 \tag{C.3c}$$

as well as the average constraint of the fields of the concentration deviations

$$\langle\tilde{c}_{A\gamma}\rangle^\gamma=0 \tag{C.3d}$$

Of all the problems studied here, the one at hand has the largest amount of sources. In this case the concentration deviations are the result of the combined effect of convective, diffusive as well as (volumetric and superficial) reactive sources. As in the previous cases studied, we formally solve this problem using standard integral equation formulations based on Green's functions, the result can be expressed as

$$\begin{aligned}\tilde{c}_{A\gamma}=&\underbrace{\left(\int_{\mathbf{y}_0\in V_\gamma}G(\mathbf{y},\mathbf{y}_0)\tilde{\mathbf{v}}_\gamma\,dV(\mathbf{y}_0)\right)\cdot\nabla\langle c_{A\gamma}\rangle^\gamma}_{\text{influence of the convective source}}\\&\underbrace{-\left(\int_{\mathbf{y}_0\in A_{\gamma\kappa}}\mathbf{n}_{\gamma\kappa}\mathcal{D}_\gamma G(\mathbf{y},\mathbf{y}_0)\,dA(\mathbf{y}_0)\right)\cdot\nabla\langle c_{A\gamma}\rangle^\gamma}_{\text{influence of the surface diffusive source}}\\&\underbrace{\times\left(-\frac{a_vk}{\varepsilon_\gamma}\int_{\mathbf{y}_0\in V_\gamma}G(\mathbf{y},\mathbf{y}_0)\,dV(\mathbf{y}_0)\right)\langle c_{A\gamma}\rangle^\gamma}_{\text{influence of the volume reactive source}}\\&\underbrace{-\left(\int_{\mathbf{y}_0\in A_{\gamma\kappa}}kG(\mathbf{y},\mathbf{y}_0)\,dA(\mathbf{y}_0)\right)\langle c_{A\gamma}\rangle^\gamma}_{\text{influence of the surface reactive source}}\end{aligned} \tag{C.4}$$

As a matter of convenience, we introduce the closure variables

$$\mathbf{f}_\gamma(\mathbf{y})=\int_{\mathbf{y}_0\in V_\gamma}G(\mathbf{y},\mathbf{y}_0)\tilde{\mathbf{v}}_\gamma\,dV(\mathbf{y}_0)-\int_{\mathbf{y}_0\in A_{\gamma\kappa}}\mathbf{n}_{\gamma\kappa}\mathcal{D}_\gamma G(\mathbf{y},\mathbf{y}_0)\,dA(\mathbf{y}_0) \tag{C.5a}$$

$$g_\gamma(\mathbf{y})=-\frac{a_vk}{\varepsilon_\gamma}\int_{\mathbf{y}_0\in V_\gamma}G(\mathbf{y},\mathbf{y}_0)\,dV(\mathbf{y}_0)-\int_{\mathbf{y}_0\in A_{\gamma\kappa}}kG(\mathbf{y},\mathbf{y}_0)\,dA(\mathbf{y}_0) \tag{C.5b}$$

in order to express Eq. (C.4) in the form given by Eq. (34), thus concluding the analysis.

## Appendix D. Consistency with other approaches

In this section we show the correspondence between our derivations for upscaling dispersion with heterogeneous reactions with those arising from other upscaling techniques. In particular, we direct our attention to the works by Edwards et al. (1993) and Mauri (1991). In the first one calculations are performed using the generalized Taylor dispersion theory and in the second one the method of homogenization is used. Both works arrive at the same effective medium equation in which the normalized effective reaction rate is an increasing function of the Damköhler number. Since the method of homogenization shares many aspects of the method of volume averaging, our analysis is based upon the work by Mauri (1991). However, the same arguments are also applicable to the work by Edwards et al. (1993).

In the work by Mauri (1991), the relation between the pointwise and the intrinsic averaged concentrations is found to

be (after neglecting higher order terms)

$$c_{A\gamma}(\mathbf{x},\mathbf{y},t) = \phi(\mathbf{y})\langle c_{A\gamma}\rangle^{\gamma}(\mathbf{x},t) + \mathbf{X}(\mathbf{y})\cdot\nabla\langle c_{A\gamma}\rangle^{\gamma}(\mathbf{x},t) \tag{D.1}$$

here $\mathbf{x}$ is a dimensionless macroscopic position vector and $\mathbf{y}$ is its microscopic counterpart in such a way that any $f(\mathbf{y})$ is periodic. In addition, the functions $\phi(\mathbf{y})$ and $\mathbf{X}(\mathbf{y})$ are analogous to the closure variables in our work. To make this point more clear, let us substitute the concentration spatial decomposition (i.e., $c_{A\gamma} = \tilde{c}_{A\gamma} + \langle c_{A\gamma}\rangle^{\gamma}$) into the above equation to obtain

$$\tilde{c}_{A\gamma}(\mathbf{x},\mathbf{y},t) = (\phi(\mathbf{y})-1)\langle c_{A\gamma}\rangle^{\gamma}(\mathbf{x},t) + \mathbf{X}(\mathbf{y})\cdot\nabla\langle c_{A\gamma}\rangle^{\gamma}(\mathbf{x},t) \tag{D.2}$$

Comparing this expression with our formal solution [see Eq. (34)], it results that

$$g_{\gamma}(\mathbf{y}) = \phi(\mathbf{y}) - 1 \tag{D.3}$$

As a matter of fact, if one substitutes this identity into Eqs. (21) of the work by Mauri (1991), the boundary-value problem for $g_{\gamma}$ [i.e., Eqs. (36a)] is recovered. Moving on to Eq. (22b) of the work by Mauri (1991), we have

$$\lambda^{*} = \frac{1}{\langle\phi\rangle^{\gamma}\mathcal{V}_{\gamma}}\int_{\mathbf{y}\in A_{\gamma\kappa}}\phi(\mathbf{y})\,dA(\mathbf{y}) \tag{D.4}$$

Substitution of the relation between $g_{\gamma}$ and $\phi$ given in Eq. (D.3) into the integral terms of Eq. (D.4) yields

$$\lambda^{*} = \frac{\mathcal{A}_{\gamma\kappa}}{\mathcal{V}_{\gamma}} + \frac{1}{\mathcal{V}_{\gamma}}\int_{\mathbf{y}\in A_{\gamma\kappa}} g_{\gamma}(\mathbf{y})\,dA(\mathbf{y}) \tag{D.5}$$

here we have taken into account the facts that $\langle g_{\gamma}\rangle^{\gamma} = 0$ and $\langle 1\rangle^{\gamma} = 1$, which is consistent with Eq. (25a) of the work by Mauri (1991). Furthermore, taking into account the definition of the interfacial area per unit volume (i.e., $a_v = \mathcal{A}_{\gamma\kappa}/\mathcal{V}$) and the porosity ($\varepsilon_{\gamma} = \mathcal{V}_{\gamma}/\mathcal{V}$), we obtain

$$\lambda^{*} = \frac{a_v}{\varepsilon_{\gamma}}\left[1 + \frac{1}{\mathcal{A}_{\gamma\kappa}}\int_{\mathbf{y}\in A_{\gamma\kappa}} g_{\gamma}(\mathbf{y})\,dA(\mathbf{y})\right] \tag{D.6}$$

Notice that the ratio $a_v/\varepsilon_{\gamma}$ corresponds to the parameter $s$ in the work of Edwards et al. (1993) (see Eq. (25) therein). Finally, from our definition of $k^{*}_{eff}$ we then conclude that

$$\lambda^{*} = \frac{a_v k^{*}_{eff}}{\varepsilon_{\gamma} k} \tag{D.7}$$

Moreover, comparing our effective medium equation with the one deduced by Edwards et al. (1993) (i.e., Eq. (6) therein), it turns out that

$$\frac{a_v k^{*}_{eff}}{\varepsilon_{\gamma}} = \overline{K}^{*} \tag{D.8}$$

or, in the notation of these authors,

$$k^{*}_{eff} = \frac{\overline{K}^{*}}{s} \tag{D.9}$$

Edwards et al. (1993) reported plots of $\overline{K}^{*}/s\overline{U}$, where $\overline{U} = \|\langle\mathbf{v}_{\gamma}\rangle^{\gamma}\|$. The correspondence between this dimensionless ratio and the definitions in this work is given by

$$\frac{\overline{K}^{*}}{s\overline{U}} = \frac{k^{*}_{eff}}{\|\langle\mathbf{v}_{\gamma}\rangle^{\gamma}\|} = \frac{k^{*}_{eff}}{k}\frac{Da}{Pe_{cell}} \tag{D.10}$$

where the Damköhler and the cell Péclet numbers are defined as

$$Da = \varphi^2 \equiv \frac{k\ell}{\mathcal{D}_{\gamma}}, \quad Pe_{cell} \equiv \frac{\|\langle\mathbf{v}_{\gamma}\rangle^{\gamma}\|\ell}{\mathcal{D}_{\gamma}} \tag{D.11}$$

Moreover, for a 2D unit cell with one squared obstacle, we have that $Pe_{\text{cell}} = (2\sqrt{1-\varepsilon_{\gamma}}/3\varepsilon_{\gamma})Pe_p$. In addition, notice that the cell Péclet resembles the Péclet number definition used by Edwards et al. (1993) and a similar comment applies for the Damköhler number. The comparison of our predictions of the effective reaction rate coefficient with those reported by Edwards et al. (1993) is available in Fig. 9.

## References


Allaire, G., Brizzi, R., Mikelic, A., Piatnitski, A., 2010. Two-scale expansion with drift approach to the Taylor dispersion for reactive transport through porous media. Chemical Engineering Science 65, 2292–2300.

Allaire, G., Raphael, A.L., 2007. Homogenization of a convection–diffusion model with reaction in a porous medium. Comptes Rendus de l' Académie des Sciences Paris, Series I 344, 523–528.

Baiker, A., New, M., Richarz, W., 1982. Determination of intraparticle diffusion coefficients in catalyst pellets—a comparative study of measuring methods. Chemical Engineering Science 37 (4), 643–656.

Balakotaiah, V., Chang, H.C., 1995. Dispersion of chemical solutes in chromatographs and reactors. Philosophical Transactions on Royal Society of London A 351, 39–75.

Balakotaiah, V., Dommeti, S.M.S., 1999. Effective models for packed-bed catalytic reactors. Chemical Engineering Science 54, 1621–1638.

Bear, J., 1972. Dynamics of Fluids in Porous Media. Elsevier.

Dadvar, M., Sahimi, M., 2007. The effective diffusivities in porous media with and without nonlinear reactions. Chemical Engineering Science 62, 1466–1476.

Edwards, D., Shapiro, M., Brenner, H., 1993. Dispersion and reaction in two-dimensional model porous media. Physics of Fluids A 5 (4), 837–848.

Eidsath, A., 1981. Flow and dispersion in spatially periodic porous media: a finite element study. Master's Thesis, UC Davis.

Eidsath, A., Carbonell, R.G., Whitaker, S., Herrmann, L.R., 1983. Dispersion in pulsed systems—iii comparison between theory and experiments for packed beds. Chemical Engineering Science 38 (11), 1803–1816.

García-Ochoa, F., Santos, A., 1994. Effective diffusivity under inert and reaction conditions. Chemical Engineering Science 49 (18), 3091–3102.

Gray, W., 1975. A derivation of the equations for multiphase flow. Chemical Engineering Science 30, 229–233.

Howes, F.A., Whitaker, S., 1985. The spatial averaging theorem revisited. Chemical Engineering Science 40, 1387–1392.

Kechagia, P., Tsimpanogiannis, I., Yortsos, Y., Lichtner, P., 2002. On the upscaling of reaction-transport processes in porous media with fast or finite kinetics. Chemical Engineering Science 57, 2565–2577.

Kolaczkowski, S.T., Ullah, U., 1989. Measurement of effective diffusivities using a spinning basket reactor. Chemical Engineering Science 44 (12), 2843–2852.

Levenspiel, O., 1999. Chemical Reaction Engineering, third ed. John Wiley and Sons.

Lichtner, P., Kang, Q., 2007. Upscaling pore-scale reactive transport equations using a multiscale continuum formulation. Water Resources Research 43 doi: 10.1029/2006WR005664.

Mauri, R., 1991. Dispersion, convection, and reaction in porous media. Physics of Fluids A 3 (5), 743–756.

McGreavy, C., Andrade Jr., J.S., Rajagopal, K., 1992. Consistent evaluation of effective diffusion and reaction in pore networks. Chemical Engineering Science 47 (9–11), 2751–2756.

Ochoa-Tapia, J., Stroeve, P., Whitaker, S., 1991. Facilitated transport in porous media. Chemical Engineering Science 46, 477–496.

Ochoa-Tapia, J.A., Stroeve, P., Whitaker, S., 1994. Diffusive transport in two-phase media: spatially periodic models and Maxwell's theory for isotropic and anisotropic systems. Chemical Engineering Science 49, 709–726.

Park, S.H., Kim, Y.G., 1984. The effect of chemical reaction on effective diffusivity within biporous catalysts—ii experimental study. Chemical Engineering Science 39 (3), 533–549.

Quintard, M., Whitaker, S., 1987. Écoulement monophasique en milieu poreux: effet des hétérogénéitéss locales. Journal de Mécanique Théorique et Appliquée 6, 691–726.

Rushton, K., 2003. Groundwater Hydrology. In: Conceptual and Computational Models. John Wiley and Sons.

Ryan, D., 1983. Effective diffusivities in reactive porous media: a comparison between theory and experiments. Master's Thesis, UC Davis.

Ryan, D., Carbonell, R.G., Whitaker, S., 1980. Effective diffusivities for catalyst pellets under reactive conditions. Chemical Engineering Science 35, 10–16.

Sahimi, M., 1988. Diffusion-controlled reactions in disordered porous media—i. Uniform distribution of reactants. Chemical Engineering Science 43 (11), 2981–2993.

Sharratt, P.N., Mann, R., 1987. Some observations on the variation of tortuosity with Thiele modulus and pore size distribution. Chemical Engineering Science 42 (7), 1565–1576.

Sperling, L., 2006. Introduction to Physical Polymer Science, fourth ed. John Wiley and sons.

Valdés-Parada, F., Alvarez-Ramirez, J., 2010. On the effective diffusivity under chemical reaction in porous media. Chemical Engineering Science 65, 4100–4104.

Valdés-Parada, F., Goyeau, B., Ochoa-Tapia, J., 2006. Diffusive mass transfer between a microporous medium and an homogeneous fluid: jump boundary conditions. Chemical Engineering Science 61, 1692–1704.

Valdés-Parada, F., Porter, M., Narayanaswamy, K., Ford, R., Wood, B., 2009. Upscaling microbial chemotaxis in porous media. Advances in Water Resources 32, 1413–1428.

Wakao, N., Smith, J.M., 1964. Diffusion and reaction in porous catalysts. I&EC Fundamentals 3 (2), 123–127.

Whitaker, S., 1999. The Method of Volume Averaging. Kluwer Academic Publishers.

Wood, B., Quintard, M., Whitaker, S., 2000. Jump conditions at non-uniform boundaries: the catalytic surface. Chemical Engineering Science 55, 5231–5245.

Wood, B., Radakovich, K., Golfier, F., 2007. Effective reaction at a fluid–solid interface: applications to biotransformation in porous media. Advances in Water Resources 30, 1630–1647.

Wood, B.D., 2009. The role of scaling laws in upscaling. Advances in Water Resources 32, 723–736.

Zhang, L., Seaton, N.A., 1994. The application of continuum equations to diffusion and reaction in pore networks. Chemical Engineering Science 49 (1), 41–50.